THE INVESTIGATION AND DEVELOPMENT OF MECHANICAL RESONANCE TISSUE ANALYSIS AND THE RELATIONSHIP TO DUAL ENERGY X-RAY ABSORPTIOMETRY AND QUANTITATIVE ULTRASOUND

by

Kyle Andrew Vernest

A thesis submitted in conformity with the requirements

for the degree of Masters of Health Science

Graduate Department of Institute of Biomaterials and Biomedical Engineering

University of Toronto

Your file Votre référence
ISBN: 978-0-494-59628-9
Our file Notre référence
ISBN: 978-0-494-59628-9

THE INVESTIGATION AND DEVELOPMENT OF MECHANICAL TISSUE RESONANCE ANALYSIS AND THE RELATIONSHIP TO DUAL ENERGY X-RAY ABSORPTIOMETRY AND QUANTITATIVE ULTRASOUND

Kyle Andrew Vernest

Masters of Health Science 2009

ABSTRACT

Currently Dual energy X-ray Absorptiometry (DXA) and Quantitative Ultrasound (QUS) are used readily in the clinical environment for the assessment of bone quality. However, neither measure is a direct mechanical measure of bone. A Mechanical Resonance Tissue Analyzer (MRTA) has been developed that looks at the ulna's deformation curve to vibration to achieve the measure of EI, cross sectional bending stiffness.

This study investigated the relationships between MRTA to that of QUS and DXA. Regression analysis found significant linear correlations between EI to BMD and BMC, however, no significant relationships were found between EI and the variables of QUS. However, this technology is seen to have a potential for the assessment of *in vivo* bone quality.

Furthermore, an improved configuration of the MRTA device is described, in addition to how preliminary results correspond to theoretical results.

Acknowledgements

I would like to thank my supervisor Dr. Angela Cheung for her generous support throughout the course of my thesis. I sincerely appreciate the opportunity she provided to me to investigate this new technology.

I am also appreciative of my committee members, Dr. Jean Zu and Dr. William Wong for lending their expertise in the various fields to my project.

Additionally, I would like to thank my program supervisor Dr. Tom Chau for his expert guidance and help in finding assistance when needed.

I would also like to thank Claudia Chan for her assistance in data collection, in addition to Queenie Wong for her analysis of DXA results, in addition to the rest of the staff in the Osteoporosis Research Program at the University Health Network

Lastly, I would like to thank my parents for their support and encouragement throughout my education.

Table of Contents:

List of Tables

List of Figures

List of Abbreviations

1/3	Distal 1/3 site of forearm
A_p	Probe effective area of contact
B	Bulk Modulus
BMC	Bone mineral content
BMD	Bone mineral density
BUA	Broadband Ultrasonic Attenuation
DEXA	Dual energy x-ray absorptiometry
E	Elastic modulus
EI	Cross sectional bending stiffness
E_s	Skin elastic modulus
F	Force
G	Shear Modulus
I	Cross sectional moment of area
ISCD	International Society of Clinical Densitometry
k_s	Skin Stiffness
L	Length
M_b	Effective mass of the beam
M_{bt}	Actual Mass of Beam
MID	Mid span site
MRTA	Mechanical response tissue analyzer
OASIS	Osteoporosis Assessment of Skeletal Integrity System
QUS	Quantitative ultrasound
ROI	Region of interest
SI	Stiffness Index
SOS	Speed of sound
SXA	Single x-ray Absorptiometry
t_s	Skin thickness
UD	Ultradistal site
V_L	Velocity of a longitudinal ultrasonic wave
WHO	World Health Organization
X	Displacement
v	Velocity
ρ	Density
ω_i	Angular frequency

Chapter 1 – Study Rational

Researchers have long been searching for the optimal method for measuring the mechanical properties of bone *in vivo*. Ultrasound and Dual energy X-ray Absorptiometry (DXA) have emerged as two leading technologies, with DXA being the gold standard for monitoring bone quality in osteoporosis. DXA has been used extensively in monitoring the effects of pharmacological agents on bone mineralization. Although the changes in Bone Mineral Density (BMD) appear to relate to changes in fracture reduction, this relationship is not significant (S. R. Cummings et al., 1993; Ettinger et al., 1999; Hochberg et al., 2002). Additionally, many researchers have found that many women that fracture have a BMD higher then usually associated with osteoporosis (Black et al., 2001; Earnshaw, Cawte, Worley, & Hosking, 1998; Karlsson, Johnell, Nilsson, Sernbo, & Obrant, 1993; Miller et al., 2004; Siris et al., 2004). As such, there is a need to better understand the mechanical properties of bone, such that fracture risk can be better predicted.

An investigational device called the Mechanical Resonance Tissue Analyzer (MRTA) was created in the mid 1980's to provide a direct mechanical measurement of bone. However, there has been some debate in the past as to its precision and accuracy in addition to the extremely low clinical uptake of this technology. This study was designed to try to understand the relationships of the current MRTA system on a clinical population of men, comparing MRTA with DXA and QUS. Additionally, development of a new device (OASIS) by our

research group using similar technology to MRTA is explained, in attempts to provide greater understanding of the fine workings of this technology and provide more precise results in the future.

Chapter 2 Introduction and Background

2.1 Bone physiology

The human skeleton provides the essential structure that humans need to work, move, and survive. In order to function properly, bone must be the correct shape, size, and strength. A lack of bone strength often results in painful and debilitating fractures, and thus bone disorders must be identified early to provide effective treatment prior to fractures. As such, physicians rely on non invasive means of quantifying bone strength.

2.1.1 Composition

2.1.1.1 Microstructure of Bone

Bone is a highly anisotropic, viscoelastic material with the ability to continually adapt to its environment. The bone matrix is a two-phase system composed of a mineral phase to provide stiffness and a non-mineralized phase consisting primarily of collagen fibers to provide ductility and absorption of energy. This multiphasic structure is similar to how rebar and concrete are combined together to produce reinforced concrete, which is stronger then the sum of the parts. Collagen is a family of proteins that are found in the extracellular matrix of connective tissues, which are essential for maintaining the structural integrity of

vertebrates and many multi-cellular organisms. Collagen is made up of three α-chains of polypeptides that form a triple helix. These collagen fibers are typically arranged in complex three dimensional structures such as concentric waves, as is found in bone (Viguet-Carrin, Garnero, & Delmas, 2006). Type-1 collagen is the most abundant in the body, and is the major protein in bone, comprising 95% of the collagen present in bone, and 80% of the total protein in bones (Viguet-Carrin et al., 2006). This collagen network provides the structure to which hydroxyapatite crystals are formed. As such, it is thought that imperfections in the collagen structure can cause subsequent bone strength problems due to improper mineralization. Hydroxyapatite is the mineralized form of calcium apatite, $Ca_5(PO_4)_3(OH)$, but is typically written as $Ca_{10}(PO_8)_6(OH)_2$ to indicate that it is in its mineralized form. This forms the component of bone that gives them their rigid structure, forming along the collagen fibers, orientated to the direction of the fibers.

2.1.1.2 Macrostructure of Bone

Bones are typically composed of two distinctive types, a hard cortical outer shell, and a complex trabecular network inside (cancellous bone).

Cancellous bone, or trabecular bone, is a highly porous osseous tissue (50% to 90% porosity) located within the cortical shell (Fisher, 2006). Due to the large porosity, trabecular bone is highly vascularized, often containing red bone marrow, which is where blood cells are produced. The majority of cancellous bone that exists within the skeleton is located within short and flat bones, as well as in the ends of long bones, near the synovial joints (Fisher, 2006). Due to its

large surface area and high level of vascularization, cancellous bone is typically more responsive to changes in mechanical loads (Fisher, 2006).

The cortical bone primary function is to provide rigid structural support to the bone for the physical demands that are often required for movement, locomotion, work, and protection of organs. The structure of the cortex is much denser in comparison to the cancellous bone, typically less then 10% porosity, and the cortical structure accounts for approximately 80% of the bone weight (Fisher, 2006). Despite this decrease in porosity, cortical bone is still very active tissue; however, it does not maintain as high a metabolic rate as cancellous bone (Fisher, 2006).

As previously mentioned, the ratio of cortical to trabecular bone varies throughout the body. Both the radius and ulna have similar distributions of mineral mass and percentage of trabecular bone to each other (Schlenker & VonSeggen, 1976). Throughout the length of the bone, the percentage of cancellous bone varies from 50% down to less than 10% at the midpoint of both bones (Schlenker & VonSeggen, 1976). Thus, at the midpoints of the bones in the forearm are composed primarily of hard cortical bone with limited trabecular structures. In the 33% region of the distal radius, it has been found that the percentage of trabecular bone is typically around 1% (Bonnick, 2004).

The percentage of trabecular bone continues to change throughout the body, varying greatly from bone to bone. As previously mentioned at the 33% site of the radius or ulna, the percentage of trabecular bone is around 1%; however, at

the calcaneous, it is around 95% trabecular bone, a stark difference (Bonnick, 2004). This is the greatest difference between commonly used peripheral and central sites of investigation in osteoporosis. Other locations that are often of interested are the lumbar spine, greater trochanter, and femoral neck with trabecular percentages of 66%, 50%, and 25%, respectively (Bonnick, 2004).

2.1.2 Bone remodeling process

Nineteenth century German surgeon Julius Wolff was one of the first to describe the dynamic properties of bone and how it is constantly changing as the demands upon it are changed. As such, it is evident that bones are not the static structure that they appear to be, rather it is in a continuous cycle of bone reabsorption and bone formation. However, it is the net balance of these two that is important as it dictates an increase or decrease in bone mass.

The cells that reabsorb bone tissue are known as osteoclasts. These are large multinucleated cells that adhere to bone in resorption pits. The osteoclasts form a sealed compartment on the pit, releasing protons into the space to create a highly acidic local environment. This low pH activates Kathepsin K, the major enzyme involved in the catabolism of bone-matrix proteins, type I and type II collagen, and osteopontin and osteonectin at low pH (Saftig et al., 1998; Bonnick, 2004).

The cells that produce new bone tissue are called Osteoblasts. These are mononucleated cells derived from osteoprogenetor cells found in the periostium and in the bone marrow. Osteoblasts produce osteoid, which is composed mainly

of type 1 collagen, forming the collagen scaffold for the hydroxyapatite. However, the mineralization is not a rapid process, and the osteoid becomes calcified over time. Often the advancing edge of the mineralized bone can sometimes trap osteoblasts, causing them to be embedded in the bone. These osteoblasts then become osteocytes and stop generating osteoid and mineralizing the matrix. These osteocytes are then believed to act as a paracrine manner of signaling to osteoblasts when experiencing mechanical loads (Hochberg et al, 2002).

This complex net interaction between bone resorption and formation within adult humans is known as remodelling. Both processes are continually going on throughout an adult skeleton. Typically, reabsorption and formation rates are similar, resulting in no significant loss in bone mass. However, when reabsorption rates exceed formation rates, bone mass is reduced.

2.1.3 Bone disorder - Osteoporosis

Though there are many bone disorders, osteoporosis affects a very large number of Canadians each year. According to Osteoporosis Canada, one in four women over the age of fifty will get osteoporosis. However, this is not only a disease that affects women, as Osteoporosis Canada also states that one in eight men over the age of fifty will get osteoporosis.

Osteoporosis can be defined as a chronic, progressively degenerative disease that is typically characterized by low bone density, micro-architectural bone deterioration, and a reduction in bone strength leading to an increase in bone fragility and correspondingly an increase in fracture risk (Mauck & Clarke, 2006).

Hip fractures are common in individuals with osteoporosis and it has been found that 50% of patients that have a hip fracture will become institutionalized and approximately 20% of those who have had a fracture will die within the first year after their fracture (Cummings & Melton, 2002). Additionally, vertebral fractures are also common and can cause chronic back pain which reduces mobility, interferes with daily activities, and leading to social isolation (S. R. Cummings & Melton, 2002).

Major risk factors for osteoporosis including age, sex, race, smoking, alcohol use, previous history of fracture, low bone mineral density, body weight, glucocorticoid use, fall risk, poor nutrition, and secondary causes of osteoporosis (Kasturi, Cifu, & Adler, 2009). It has been found that as individuals get older they are at a greater risk of fracture, even with the same bone mineral density (Gardner et al., 2005). In comparison to men, women have smaller bones, which puts them at greater risk of fracture (Gold & Silverman, 2004). In addition to sex, race is another factor that contributes to an individual's risk of osteoporosis, with white people from countries closer to the two poles having a greater risk. Smoking has been found to increase free radical mediated injury and decreasing calcium absorption (Bogoch et al., 2006). Similarly, having more than two units a day of alcohol has been found to increase the risk of osteoporotic fractures (Zerwekh, Ruml, Gottschalk, & Pak, 1998). Moreover, people who have had a personal history of fracture increase their risk by two to three times, where as those who just have a family history of fracture only has a modest, yet still a significant increase in risk (Ramnemark, Nyberg, Lorentzon, Englund, & Gustafson, 1999;

Zehnder et al., 2004). Furthermore, individuals with low body mass typically have an increased risk due to decreased loading resulting in a lower peak bone mass, and less fatty tissue to protect the bones when falling (Alenfeld et al., 2000). Similarly, low bone densities have been shown to be associated with an increased risk of fracture (Black et al., 1992; S. R. Cummings et al., 1993; S. R. Cummings & Melton, 2002; Nevitt et al., 1994; Stone et al., 2003). Glucocorticoids have also been shown to decrease bone formation and increase in bone resorption, resulting is significantly lower bone densities (Peel, Moore, Barrington, Bax, & Eastell, 1995). Those at an increased risk of falling also have a higher prevalence of fracture (S. R. Cummings et al., 1995). Lastly, poor nutrition can result in lower levels of Vitamin D and Calcium, in addition to lower body mass, and lower peak bone mass, all predisposing an individual to osteoporosis.

Additionally, there are many secondary causes of osteoporosis. Some of the more prevalent secondary causes are presented in Table 1.

Table 1 - Secondary Causes of Osteoporosis (Adapted from (Fitzpatrick, 2002**))**

Endocrine disorders
Cushing syndrome
Eating disorders
Endometriosis
Gonadal insufficiency (primary or secondary)
Hyperparathyroidism
Hyperthyroidism
Hypogonadism
Nutritional disorders
Tumor secretion of parathyroid hormone–related peptide
Gastrointestinal disease
Alcohol-related liver diseases
Celiac disease

Chronic active hepatitis Chronic cholestatic diseases Gastrectomy Inflammatory bowel disease Jejunoileal bypass Malabsorption syndromes Severe liver disease **Marrow-related disorders** Leukemia Lymphoma Multiple myeloma **Organ transplantation** Bone marrow Heart Kidney Liver Lung **Miscellaneous causes** Idiopathic hypercalciuria Idiopathic scoliosis Multiple sclerosis Rheumatoid arthritis Genetic disorders Osteogenesis imperfecta

2.2 In vivo bone quality measurement techniques

2.2.1 DXA

Dual Energy X-ray Absorptiometry (DXA) is the current standard utilized in their definition of osteoporosis. The World Health Organization (WHO) defines Osteoporis as having a DXA BMD T-score -2.5 standard deviations or lower the a young health adult population. This is one of the most popular methods of qualifying bone properties due to the fairly well established relationship between bone mineral density (BMD) and fracture risk (Black et al., 1992; S. R. Cummings et al., 1993). DXA provides a quantitative measure of the mineralization level in

bone; however, it does not address the entire complex multiphasic structure, including things such as collagen and proteins.

2.2.1.1 Principals

The fundamental principle for DXA is the measurement of the transmission of x-rays through the body at high and low energies. X-rays travel through the body they will either pass through unaffected (transmission), be absorbed, or are scattered into the environment. For a given thickness, attenuation increases with an increase in density. Similarly, for a given density, attenuation increases with increasing thickness. However, different materials have different absorption at different energies, and it is this principle that allows DXA to be more effective than Single X-ray Absorptiometry (SXA). By using two different energies (140KVp and 70KVp), that have different absorption spectrums, two equations for the curve can be simultaneously solved, to determine the bone density at each point (Blake & Fogelman, 1999). This creates a pixel by pixel map of the BMC for the area scanned. Edge detection algorithms are then used to determine the edge of each bone as a boundary of where to calculate BMC. The BMC is determined by taking the average value for each pixel. BMD is then calculated by taking BMC and dividing by the area, determined as the number of pixels in the ROI. Since the x-rays are projecting through the plane to provide a 2D image, the BMD is actually an areal bone mineral density, in units of g/cm^2, rather than true BMD, which would be in g/cm^3, something that is now possible with Quantitative Computed Tomography (QCT).

First general DXA scanners utilized a pencil beam x-ray source combined with a single detector in the scanning arm. Most common DXA machines now utilize a fan beam x-ray source, which uses a slit collimator to generate a fan beam which is then coupled to a linear array of detectors in the scanning arm (Blake & Fogelman, 1999). This allows the generator to move along one axis collecting data much more rapidly than the pencil bean which must move back and forth in addition to moving along the long axis. These two technologies are illustrated in Figure 1.

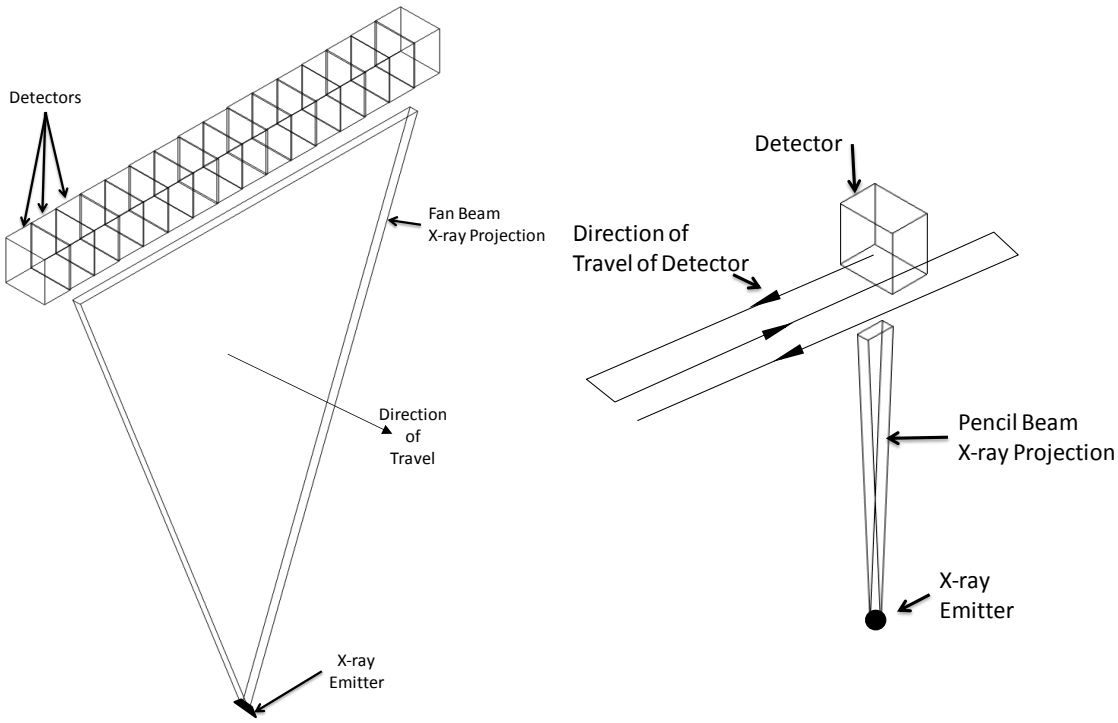

Figure 1 - principle pixel collection for DXA. The left image illustrates the modern fan beam, where as the right illustrates the pencil beam method

In addition to BMC and BMD, there are two other common ways in which results are presented: T-scores and Z-scores. A T-score is the relationship of the BMD to a young healthy population in the number of standard deviations. Thus, a T-

score of -1.0 means that the individual's BMD is one standard deviation below a young healthy population. Z-score on the other hand is a relationship of BMD to an aged matched population. Thus, a Z-score of -1.0 would mean they are one standard deviation below people at their age.

2.2.1.2 Clinical use

With the widespread use of DXA, large data sets have been compiled on DXA data, allowing for improved data and increasing number of relations. Now T-scores and Z-scores can be race matched as well. However, this also provides increasing difficulty for mixed races. An individual who has an African American mother and Caucasian father, would fall somewhere in between. As such, there is still work being done to improve databases that are used, such that increasingly relevant data can be obtained. As such, the International Society for Clinical Densitometry (ISCD) recommends matching everyone to Caucasian; however this is not always followed in clinical settings.

The lumbar spine is often used to monitor response to treatment due to the large proportion of cancellous bone in each vertebra, resulting in a high surface area, and thus highly active bone tissue (Blake & Fogelman, 1997). However, there are issues that can affect these scans, causing inaccuracies in the results. Compression fractures that occur in the lumbar spine give the illusion of higher BMD due to the same amount of BMC distributed over a smaller area, decreasing the accuracy of the readings. Additionally, since the scan is a projection through the body, things such as aortic calcification can cause increased x-ray attenuation, skewing the results (Blake & Fogelman, 1997).

DXA is also used to monitor an individual's progress in their treatment of osteoporosis. Many centers have individuals identified as being osteoporotic return for scans every one to two years to monitor their response to treatment. This allows a health care provider to ensure the patient's bone health is either improving or not getting worse, and provides appropriate feedback to the patient.

Currently there are only two limiting factors for a patient not to receive DXA scans. If a woman is pregnant, there is concern with regards to exposure to the ionizing radiation for the developing fetus, and as such they should not receive BMD scans. The second limiting factor is an individual's weight. Many tables have weight limits imposed on them to prevent damage to the table. In very obese people, their weight may exceed the limitation of the tables, limiting their ability to have a BMD.

2.2.1.3 Bone quality and DXA Studies

Bone mineral density is not the only factor in whole bone quality. It is estimated that BMD makes up approximately 70% of total bone strength, and other factors such as collagen fiber orientation & cross-linking, trabecular connectivity, micro fractures, and endosteal porosities constitute the remaining fraction of bone strength (Martin, 1991).

Nevertheless, there is a well established relationship between BMD and fracture risk (Black et al., 1992; S. R. Cummings et al., 1993). In a meta-analysis of 12 large randomized, blinded trials of antiresorptive drugs in postmenopausal women, Cummings et al. found that a 1% improvement in spine BMD was

associated with a 0.03 decrease in the relative risk of vertebral fracture (S. R. Cummings et al., 2002). A similar study by Hochberg et al., completing a meta-analysis of 18 studies of antiresorptive drugs found a 1% increase in spine BMD one year after starting resulted in an eight percent reduction in non-vertebral fracture risk (Hodgeberg et al., 2002).

However, in a study of 8065 women age 65 and older by Wainwright et al., found that 54% of participants who had fracture, where not classified as osteoporotic by the WHO at the start of follow-up (Wainwright et al., 2005). Additionally there is a growing number of studies that suggest many women who fracture have BMD higher than that normally associated with osteoporosis (Black et al., 2001; Black et al., 2001; Earnshaw et al., 1998; Karlsson et al., 1993; Schott et al., 1998; Stone et al., 2003). As such, though a relationship to fracture is somewhat established, there is still no consistent way of determining mechanical loading noninvasively, and thus when an individual will fracture.

2.2.2 QUS

2.2.2.1 Principals

The speed at which ultrasonic waves passes through a given material depends on the properties of that material, both elasticity and density, and its mode of propagation (Pain, 2005). Since most ultrasound measurements are taken on the heel (calcaneous), the lateral dimension of the bone is not significantly smaller then the wavelength. As such, the velocity (V_L) of a longitudinal wave is propagated as:

$$V_L = \sqrt{\frac{B + \frac{4}{3}G}{\rho}}$$ **(1)** (Njeh, Fuerst, Diessel, & Genant, 2001)

where B is the Bulk Modulus and G is the Shear Modulus. Thus, the Speed of Sound (SOS), which is the distance between emitter and receiver, divided by the time it takes for the signal to travel though the bone, is dependent on the elasticity and density of the bone.

Similar to DXA, when sound waves travel through bone they can be absorbed and/or scattered, resulting in a decrease in amplitude. The amount of scattering that occurs is proportional to a number of internal factors, such as the internal structure and acoustic properties of the medium (Njeh et al., 2001). Though bone mass accounts for some parts of scattering and signal attenuation, the architecture of the bone is said to account for a much greater part of this signal (Kaczmarek, Pakuła, & Kubik, 2000). This technique of measuing the attenuation of the signal is referred to as Broadband Ultrasound Attenuation (BUA), and is often measured in conjunction to SOS measurements.

The Ultrasound signal is typically both generated and transduced by piezoelectric transducers. The one piezoelectric transducer emits a signal, typically between the 200 to 800 kHz range, producing wavelengths 2-8mm. The other piezoelectric transducer receives the signal which is the converted to a voltage and analyzed. Since the distance between the sensors is typically fixed the time from signal initiation to receipt can be measured and SOS calculated.

2.2.2.2 Clinical use

Though not used in North America as extensively as DXA, in nations with limited access to DXA machines, QUS has become the standard measurement of quantitative bone quality. This is primarily due to the much lower cost of QUS machines versus DXA machines. Additionally, there is less training required to use QUS machines than the much more complicated DXA machines. Additionally, DXA machines utilize ionizing radiation which makes it inherently more dangerous when repairing. As such, QUS is inherently more affordable than DXA, however, the use of QUS for diagnosis of bone disorders is debated (Fogelman & Blake, 2000).

2.2.2.3 Bone quality and QUS studies

Several studies have illustrated that there is a strong link between BUA and BMD (Duquette, Honeyman, Hoffman, Ahmadi, & Baran, 1997; Han, Rho, Medige, & Ziv, 1996; Langton, Njeh, Hodgskinson, & Currey, 1996; Nicholson, Haddaway, & Davie, 1994; Serpe & Rho, 1996). However, the ultimate goal is the relationship between QUS and the mechanical structural properties of bone, as this is what is indicative of fracture risk.

There have been several studies that have looked at the ability of QUS to determine the mechanical properties of bone. In a study by Ashman et al., they found that the modulus of elasticity measure with QUS and mechanical testing to be highly correlated, having an R^2 value of 0.935 (Ashman, Corin, & Turner, 1987). In a somewhat similar study by Njeh et all, the correlation between bone elasticity and velocity was found to have a R^2 value of 0.794 in the proximal distal

plane, 0.829 in the anterior posteriors plane, and 0.805 in the medial lateral plane of bovine femurs (Njeh, Hodgskinson, Currey, & Langton, 1996). These studies and others are summarized in Table 2 and illustrate a relatively high correlation to bone strength.

Table 2 - relationship between Young's Modulus (E) and specified QUS variables

Study	Bone	Variable(s)	Mode	R^2
(Ashman et al., 1987)	Human calcaneous	velocity	linear	0.935
(Langton et al., 1996)	Human calcaneous	BUA	log	0.76
(Njeh et al., 1996)	Bovine femur	velocity	Log	0.83
(Hodgskinson, Njeh, Whitehead, & Langton, 1996)	Bovine femur & human calcaneous	Density, Velocity, BUA	log	0.98
(Bouxsein & Radloff, 1997)	Human calcaneous	BUA	log	0.64

As illustrated in Table 2, there are many ways in which QUS values can be related to modulus of elasticity (E) and with varying results. The relationship between QUS and bone structure / fracture risk is not nearly as well established as DXA nor is its clinical use as widespread. As such, many researchers decipher QUS results with caution.

Chapter 3 Vibration analysis of bone and the development of MRTA

3.1 Historical Development

Initial work on mechanical impedance of bones in the body as a means of quantifying their mechanical properties initially began with investigators looking at the human skull. Impedance methods were already used in the investigation of mechanical and acoustical vibrations; however, in the early 1950s Franke began applying this technique in the investigation of the impedance of vibrational

signals on the human body (Franke, 1951). It was found that the mechanical response to vibration could be used to calculate the stiffness constant of muscle or bone (Franke, 1951; Franke, 1952; Franke, 1956). Additional initial investigations looked at several different parameters of bone's attenuation to vibration, looking at nodal lines or the frequency response at different distances from the receiver, the velocity of propagation of vibrational waves, and the attenuation to vibration (Franke, 1956).

Later studies, continue from this primary work, looking at the complex impedance (Campbell & Jurist, 1971; Christensen et al., 1986; Collier, Nadav, & Thomas, 1982; Franke, 1952; Hodgson, Nakamura, & Nakamura, 1968; Jurist & Kianian, 1973; Thompson, Young, & Orne, 1976; D. R. Young, Howard, Cann, & Steele, 1979; D. R. Young, Niklowitz, & Steele, 1983) and/or the vibratory impact response (Christensen et al., 1986; Lewis, 1975; Saha & Lakes, 1977) of bones to try and determine mechanical properties. Impulse studies examined the application of a quick impulse to the bone, such as with a gently hammer strike or an air driven pellet and measuring the response to this impulse with an accelerometer manually pressed on the bone distal to the impulse. In the initial impact study, by Lewis (1975), he initially just looked at the peak magnitudes and frequency of the accelerometer signal between fractured and non-fractured bones. However, he noted that complex stiffness would likely be a better measure of these changes in frequency and magnitude. Thus, in the studies by Saha & Lakes (1977) and Christensen et al (1986), the complex impedance measures were used to evaluate the *in vivo* properties of bone. To achieve the

complex impedance, force and velocity signals are Fourier transformed and dividing the transformed force by velocity , yielding the transfer function of the system. Often this is repeated at several points on the long bone such that the bone can be adequately characterized. However, a difficulty with using resonate frequencies as a quantification of bone is that resonate frequencies in vibrating systems depend on the ratio of stiffness to mass (Thompson et al., 1976). This is significant as a bone which has reduced carrying capacity, would likely have both reduced stiffness and mass, but would appear to have normal resonate frequency characteristics.

Impedance studies are more numerous and appear to provide greater insight into bone properties; however, they are more difficult to undertake and take a longer period of time. These studies analyzed the response over a large frequency range, using a range of discrete frequency applications (Campbell & Jurist, 1971; Franke, 1951; Franke, 1952; Franke, 1956; Hodgson et al., 1968; Thompson et al., 1976; D. R. Young et al., 1979; D. R. Young et al., 1983) or a swept sine wave (Christensen et al., 1986; Collier et al., 1982; Noyes, Clark, & Watson, 1968) . Both methods work very similarly, however the swept sine wave required more sophisticated hardware, such as a harmonic analyzer. The discrete frequency method however could be completed with the simplest of equipment, such as an oscilloscope, measuring the magnitude and phase shift for each frequency. Early research using the impedance method on bone by Franke utilized the complex impedance method for looking at results, as this provided a way to interpret the results independent of the force, amplitude, or frequency

applied (Franke, 1951; Franke, 1952; Franke, 1956). This technique was carried through to subsequent research. However, Thompson et al. (1976) utilized a mathematical model in the analysis of human ulna. This is an essential part because resonate frequencies depend on the ratio of stiffness to mass, and if both are reduced it causes no change in the resonate frequency. Thus, by modeling the bone as a long beam can overcome this issue, and provide a singular value of cross sectional bending stiffness for the isolated frequency spectrum. However, the modeling proposed here still required radiographic data, such as BMC per unit length and bone width, or other such estimated data to fulfill missing requirements of the model.

3.2 MRTA Development

Prior to the work by Steele et al. in 1988, the long bone EI was determined using the first mode of free vibration. This methodology and framework is outlined here. This model focused on the lower frequency response, where in long bones the first bending mode is dominant.

Previously, Cornelissen et al. (1986) has reported that the “skin,” being all soft tissue between the impedance transducer and the bone, had little effect on the mode of vibration, the general shape. However, it was found that it does significantly modify the impedance measurement at the skin. Additionally, it was found that the skin and bone behave as two springs in series (Steele et al., 1988). As such, it was established that:

$$k_s = \frac{F}{x} = \frac{E_s A_p}{t_s}$$ **(2) (**(Steele et al., 1988)

where k_s is the stiffness of the "skin", F is the resultant force, x is the displacement, E_s is the skin elastic modulus, t_s is the skin thickness, and A_p is the probe effective area in contact with the limb. Additionally, it is known that the lateral stiffness, k_b, of a simply supported uniform beam loaded at the midpoint is:

$$k_b = \frac{48EI}{L^3} \quad \textbf{(3)} \text{ (Steele et al., 1988)}$$

where E is the elastic modulus of the beam, I is the cross-sectional moment of inertia of the beam. The ultimate goal is to determine EI, the product of the elastic modulus of the beam and the cross-sectional moment of inertia, which can be approximated once the stiffness is delineated.

The frequency of the first mode of free vibration for a uniform beam that is simply supported is defined by:

$$f = \frac{\omega}{2\pi} = \frac{1}{2\pi}\left(\frac{EI}{\rho A}\right)^{\frac{1}{2}}\left(\frac{\pi}{L}\right)^2 \quad \textbf{(4)} \text{ (Steele et al., 1988)}$$

where f is the frequency in Hz of the first node, ρ is the density of the beam, and A is the cross-sectional area. Thus, we can also define the total mass of the beam, M_{bt}, from these variables:

$$M_{bt} = \rho AL$$

Equation (4) can be rewritten to include equation (2) expressed for bone stiffness, equation (5) and which yields:

$$f = \frac{1}{2\pi}\left(\frac{k_b}{M_b}\right)^{\frac{1}{2}}$$ **(5) (**(Steele et al., 1988)**)**

However, M_b is the effective mass of the beam, rather then the actual mass of the beam, M_{bt}. This can be converted to the actual mass for center midpoint loaded simply supported uniform cross sectional beams as follows:

$$M_b = \frac{48}{\pi^4} M_{bt} = 0.493 M_{bt}$$ **(6)** (Steele et al., 1988)

Steele et al. presented a new, novel approach to the modelling scenario that did not require the use of external or radiographic properties (with the exception of limb length), which essentially allowed this device to operate independently of any other (Steele et al., 1988). This utilized a seven-parameter model for the response curve.

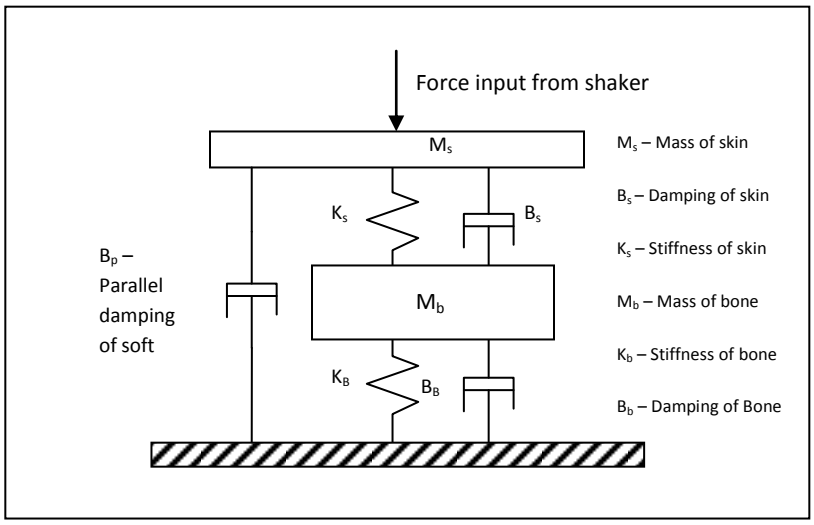

Figure 2 - 7 Parameter model for vibratory response in a long bone

The stiffness transfer function, force divided by displacement, is used as the transfer function as it provides more consistent results than impedance curve, force over velocity (Steele et al., 1988). Using a curve fitting program poles and zeros are used to obtain the best fit of both the real and imaginary parts of the stiffness transfer function. The seven parameter model, illustrated in Figure 2, has a complex stiffness that is defined by the equation:

$$\frac{F}{x} = M_s \frac{s^4 + A_3 s^3 + A_2 s^2 + A_1 s + A_0}{s^2 + C_1 s + C_0} \quad \textbf{(7)}\ \text{(Steele et al., 1988)}$$

The equations to describe the coefficients of the physical parameters and non-linear relations are described by Steele et al. (1998).

Once the bending stiffness of the bone is known, it can then be applied to equation 2 to determine the cross sectional bending stiffness.

Chapter 4 Materials and Methods

4.1 Study Population

Fifty-eight participants, all men, over the age of 35 were recruited for this study. Subjects were excluded if they have had fractures in both arms, as this would limit them from having BMD and MRTA readings. All subjects agreed to participate in the MRTA, QUS, and DXA procedures. The study was approved by the University Health Network Research Ethics Board, Toronto, Canada and written informed consent was obtained from each participant prior to their participation in the study.

4.1.1 Procedures

4.1.1.1 DXA

One Hologic Discovery A densitometer (Hologic Inc., Waltham, MA) was used to perform the DXA scans of the spine, hip, and forearm. Standard hip and spine regions of interest (ROIs) were used, with BMC, BMD, and projected area were measure and recorded for each site. The forearm ROIs consisted of: the ultradistal site (UD) beginning 10mm proximal to the ulnar styloid process, extending proximally 15 mm; the 33% region, a 20mm region centered around the distal one-third point of the ulna length; and the midspan region, a 20 mm region centered around the midpoint of the ulna. The regions of interest are illustrated in Figure 3. The subject's non-dominant forearm was used unless they had experienced a previous fracture on the humorous, tibia, or radius of that arm. All measurements were collected and processed by 2 experienced bone density technologists in a research hospital setting. Quality controls were preformed daily on the densitometer according to the manufacturer's specifications using a spine phantom. The coefficient of variation for BMD on the machines is 1.0%.

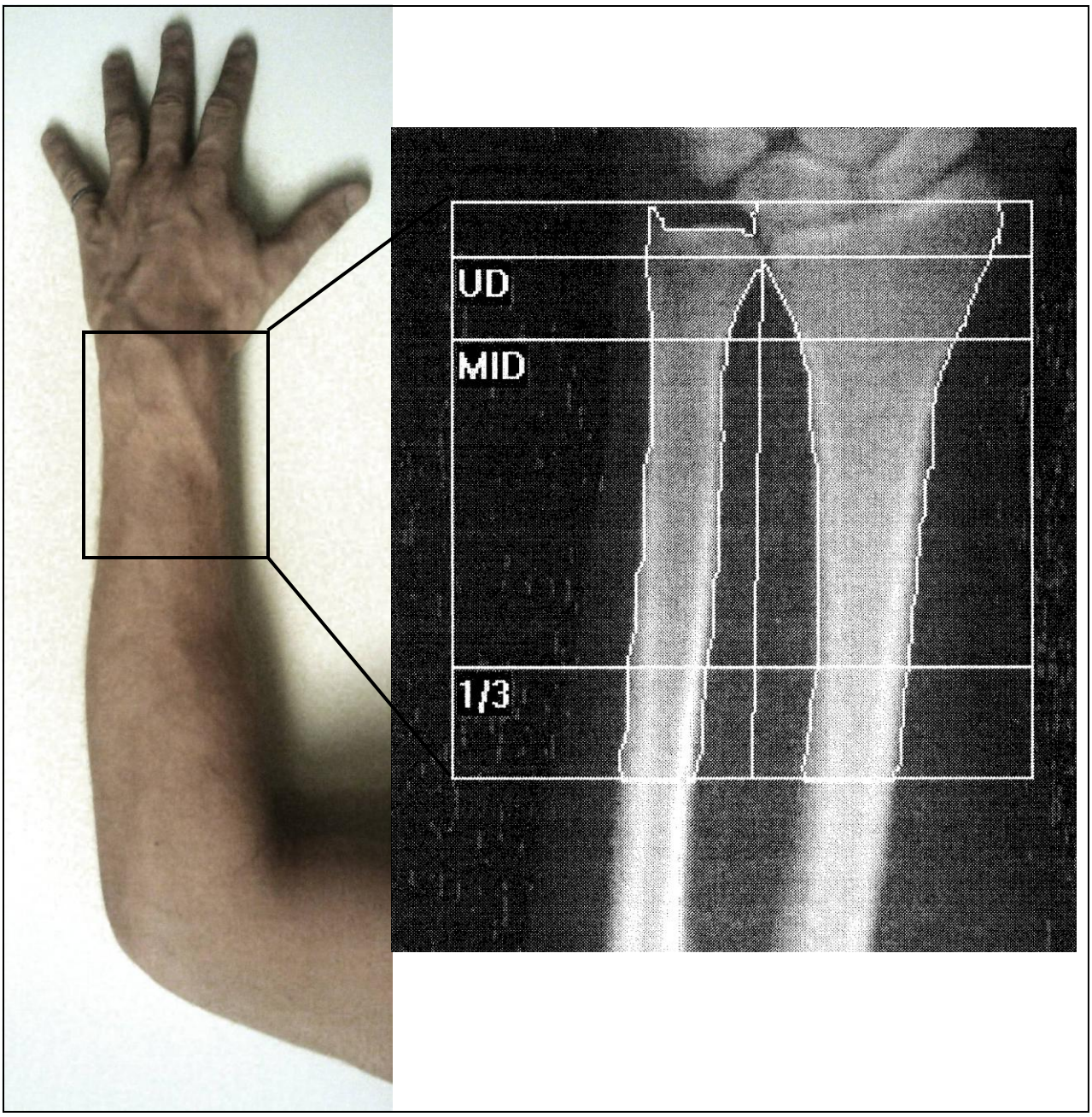

Figure 3 - Regions of Interest (ROI)s of the forearm: UD = Ultradistal Site, MID = midspan region, 1/3 = Distal 1/3 region.

4.1.1.2 QUS

A GE Achillies Expresses (GE Healthcare, USA) was used to perform quantitative ultrasound scans of the calcaneous. Subjects were seated in a chair and then place their heel into the machine, with the toe alignment probe placed

between the first and second toe to ensure proper alignment of the foot and ankle. Additionally, the chair was positioned such that there was no rotation of the ankle. A solution of 90% isopropyl alcohol was sprayed onto the ankle just as the machine was initialized to help improve signal conduction and sanitization. The speed of sound (SOS), broadband ultrasound attenuation (BUA) and stiffness index (SI) were collected by an individual in our institution experienced with heel ultrasound measurement. Quality controls were performed daily on the QUS device using a heel phantom in accordance with the manufacturer's specification. The device used has a coefficient of variation of 2% for all measurements.

4.1.1.3 MRTA

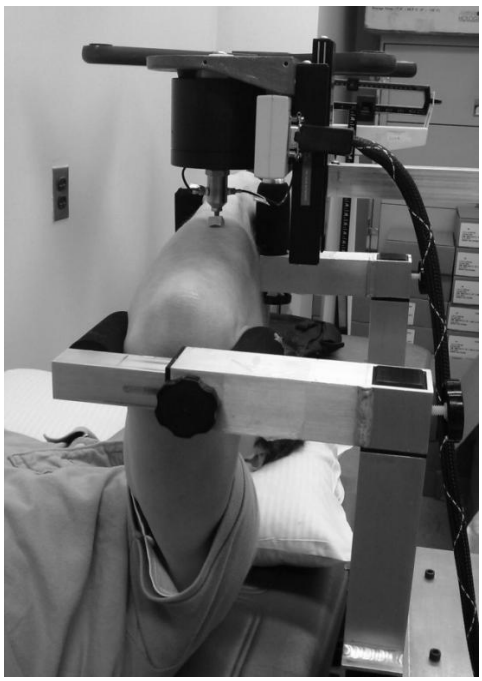

Figure 4 - Sample MRTA setup

MRTA tests were performed with all subjects supine on a medical examination table, using a GaitScan MRTA. The same arm that was assessed for the forearm BMD was placed within the supports of the MRTA, with the elbow and wrist immobilized within the cushioned supports. The arm was positioned such that the ulna and radius were parallel with the floor and the humorous was perpendicular to the floor, as illustrated in Figure 4. While the arm was positioned within the supports, the length of the ulna was obtained by measuring the distance from the styloid process to the distal end of the olecranon process. The midpoint was determined by marking half the distance with an ink pen, to allow proper positioning of the MRTA probe later. Before the probe was placed upon the ulna, subjects were warned to expect the probe to be heavy and that they should not tense or flex their arm, trying to keep it as relaxed as possible. When the subject was ready the probe was positioned on the previously marked midpoint. After the measurement had finished the probe was removed from the subjects arm; however, the subjects arm was left in the supports. The operator then repositioned the probe and collected another measurement. Additional collections were completed at the operator's discretion from their previous experiences with MRTA data collection. Quality controls were performed each day on an aluminum rod of known cross-sectional bending stiffness.

In addition to the 7parameter GaitScan value determined on the machine, four other models were calculated using the transfer function from the MRTA. These four other models included a modified seven parameter, a twelve parameter, a six parameter, and a nine parameter model.

Chapter 5 Results & Discussion

5.1 Results

5.1.1 Summary of participants

The characteristics of the subjects are presented in Table 3 as the mean ± standard deviation.

Table 3 - Subject Characteristics

n	Weight (kg)	Height (cm)	Age (years)	Waist (cm)	Ulna Length (cm)
58	85.59 ± 17.16	176.47 ± 6.39	51.3 ± 10.7	100.46 ± 13.69	2733 ± 1.2

5.1.2 EI Quality Controls

It was found that the Gaitscan EI values were the most consistent for the quality control rods. As such, the Gaitscan EI was used as the primary means of correlation to MRTA EI.

5.1.3 EI Linear Regression Analysis

Eighty-eight variables were recorded for each individual over four categories, physical measurements, DXA measurements, MRTA measurements, and QUS measurements. In addition to these 88 measurements, the square of each measurement was also introduced. These 176 variables, were used in a linear regressions in combinations of every other measurement, such that 30800 regressions were performed. This was possible using a custom written script using MATLAB 7.0.1 (Mathworks, Natick, Massachusetts). The highest R^2 value of the four options (x vs. y, x^2 vs. y, x vs. y^2, or x^2 vs. y^2) was selected as the best representation for that pair. This was completed to see if any other relationships

existed other than the ones expected; however, no supplemental relationships of significance were noted.

Several of the physical measurements had correlations between themselves. However, many of these were to be expected, such as height relates well to waist size, and both relate well to an individual's weight. Height and bone length also seemed to correlate well to each other.

Each of the groups of measurements also seemed to have relatively high correlations to each other. All EI calculations correlated significantly to each other, however often the R^2 value was not very high for these correlations, indicating that each model was accounting for slightly different properties. The modified 7parameter value correlated the best to the Gaitscan EI, with a R^2 value of 0.9486, and a p-value of 0.

The BMD results of one Region of Interest (ROI) correlated fairly highly with the other BMD ROI results. Most of the correlations were significant, however, some correlated better than others. Measures from similar areas correlated very strongly together, such as the area of L1 with the area of L2 or L3, and as such there were fairly good correlations between properties such as area of L1 and BMD of L3. There was less correlation between different ROIs in the body, such as the BMC of the greater trochanter and the area of distal radius, however many of these relationships were still found to be significant.

With QUS, all variables had significant correlations with the other QUS measurements, with the exception of the SOS of the right calcaneous. The other

values correlated fairly well to each other, with all R^2 values of significant correlations being greater than 0.5.

The results of interest in relation to the Gaitscan EI are presented in Table 4 with their corresponding R^2 and p-value for significance. Significance was analyzed at $p<0.05$, and these values are highlighted in bold text.

Table 4 - linear correlation between the Gaitscan EI and other measures of interest. Significant Correlations (P<0.05) are in bold.

Relationship	R^2 Value	P -value
$(EI)^2$ vs. $(Age)^2$	0.00466	p=0.831
$(EI)^2$ vs. $(Weight)^2$	0.00276	p=0.79824
EI vs. Height	**0.09438**	**p=0.018991**
EI vs. Waist	0.00738	p=0.5215
EI vs. $(Hip\ Size)^2$	0.00155	p=0.76934
EI vs. $(Bone\ Length)^2$	**0.10152**	**p=0.014786**
EI vs. Average EI - 7Parameter	**0.94860**	**p=0**
EI vs. Average EI - 6Parameter	**0.83270**	**p=0**
EI vs. Average EI - 9Parameter	**0.32172**	**p=0.0000034442**
EI vs. Average EI-12Parameter	**0.14327**	**p=0.0033924**
$(EI)^2$ vs. Left BUA Average	0.05476	p=0.077074
$(EI)^2$ vs. Right BUA Average	0.01975	p=0.2927
$(EI)^2$ vs. Left SOS Average	0.01091	p=0.43521
$(EI)^2$ vs. Right SOS Average	0.01252	p=0.40297
$(EI)^2$ vs. Left SI Average	0.03034	p=0.19095
$(EI)^2$ vs. Right SI Average	0.01658	p=0.33544
$(EI)^2$ vs. $(Total\ Spine\ Area)^2$	0.11453	p=0.74029
EI vs. Total Spine BMC	**0.10143**	**p=0.014831**
EI vs. Total Spine BMD	0.03216	p=0.17799
$(EI)^2$ vs. $(Radius\ 1/3\ BMC)^2$	0.36643	p=0.16048
$(EI)^2$ vs. $(Radius\ 1/3\ BMD)^2$	0.04111	p=0.88054
EI vs. Ulna 1/3 Area	**0.46164**	**p=0.0000000045221**
$(EI)^2$ vs. $(Ulna\ 1/3\ BMC)^2$	0.37906	p=0.225
$(EI)^2$ vs. $(Ulna\ 1/3\ BMD)^2$	0.05638	p=0.49895
$(EI)^2$ vs. $(Ulna\ Midspan\ BMD)^2$	0.27619	p=0.35654
$(EI)^2$ vs. $(Ulna\ Ultradistal\ BMD)^2$	0.00092	p=0.95498
EI vs. Total Radius Area	**0.33796**	**p=0.0000017086**

EI vs. Total Radius BMC	**0.28597**	**p=0.000015304**
$(EI)^2$ vs. Total Radius BMD	0.00763	p=0.51438
$(EI)^2$ vs. $(Total\ Ulna\ Area)^2$	0.48800	p=0.16626
$(EI)^2$ vs. $(Total\ Ulna\ BMC)^2$	0.29903	p=0.24342
$(EI)^2$ vs. Total Ulna BMD	0.01933	p=0.29789
$(EI)^2$ vs. $(Total\ Radius\ \&\ Ulna\ BMC)^2$	0.41448	p=0.30161
$(EI)^2$ vs. $(Total\ Radius\ \&\ Ulna\ BMD)^2$	0.05564	p=0.3837
$(EI)^2$ vs. $(Total\ Hip\ BMC)^2$	0.13707	p=0.42188
$(EI)^2$ vs. Total Hip BMD	0.00115	p=0.80045
$(EI)^2$ vs. $(Hip\ T\text{-}score)^2$	**0.01677**	**p=0**

5.1.3.1 EI correlation with Age

The correlation between the Gaitscan EI and participant age is illustrated in Figure 5. This relationship is non-significant, and has a low level of correlation.

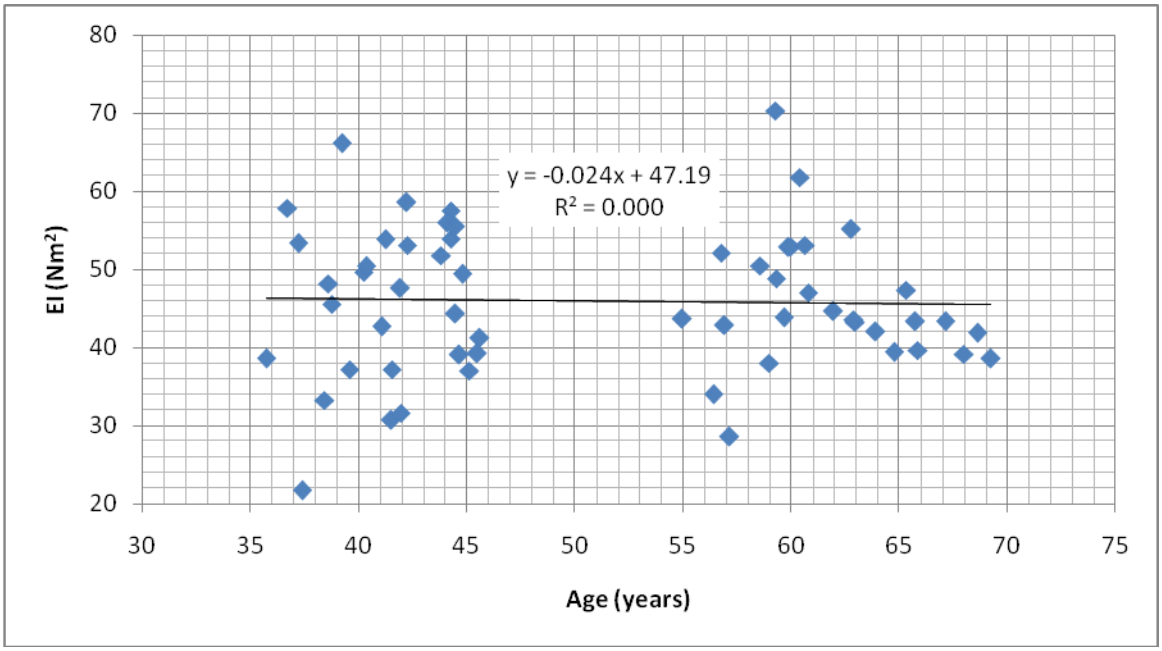

Figure 5 - (Non-significant (p=0.813) Linear regression between EI and Age

5.1.3.2 EI correlation with Ulna

5.1.3.2.1 1/3 Distal Ulna

The correlations with the DXA results for the 1/3 distal region of the ulna is the ROI of the wrist that is in closest approximation to the physical location of the ulnar midpoint, where the MRTA probe vibrates the ulna. The relationship between $(EI)^2$ and $(BMD)^2$ at this area had the highest R^2 value of the four scenarios, as presented in Figure 6; however none provided significant correlations. The best (and significant) correlation occurred between the area of the region and the EI value as illustrated in Figure 7.

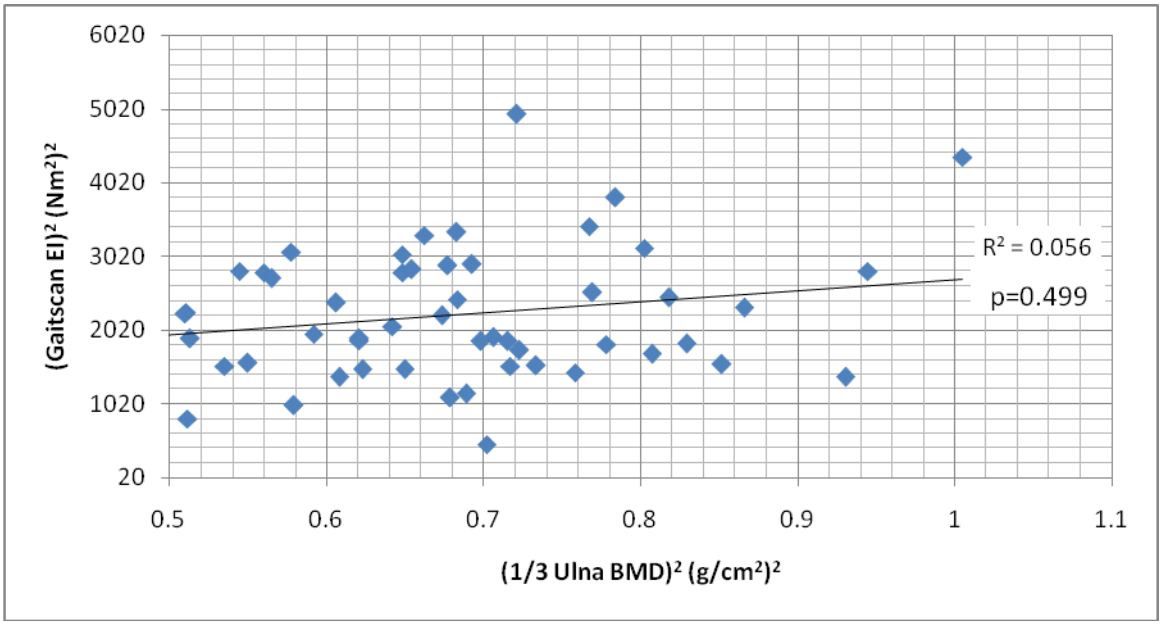

Figure 6 - (Non-significant) linear regression between $(EI)^2$ and $(BMD)^2$ at the 1/3 distal ulna

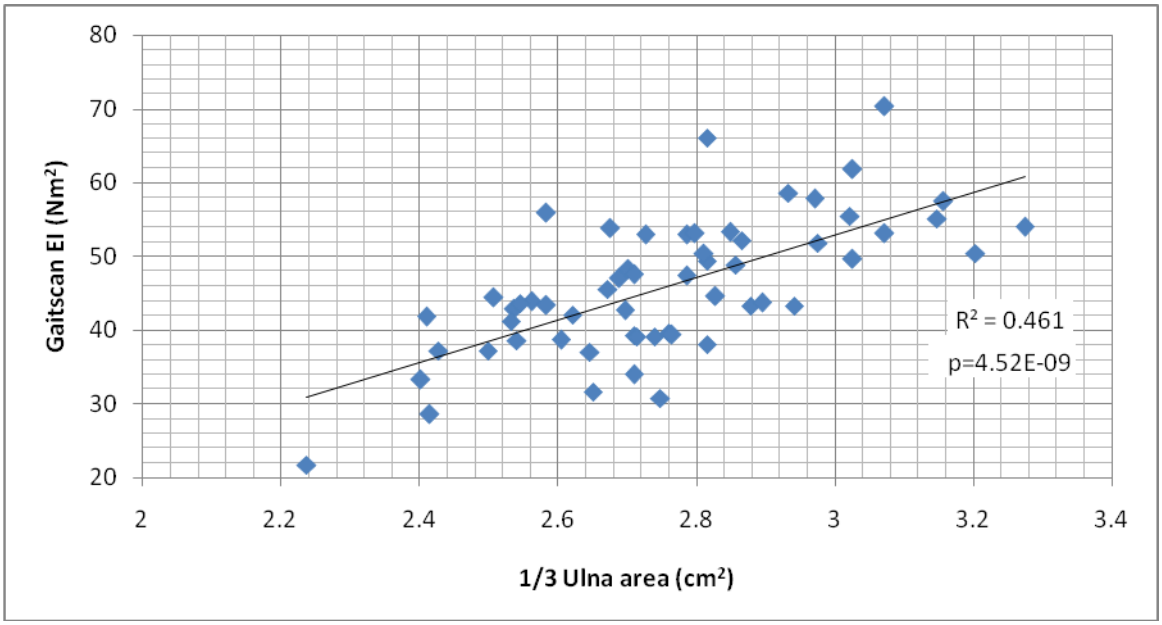

Figure 7 - Linear regression between EI and area of 1/3 distal region of ulna

5.1.3.2.2 Total Ulna

The regressions for the total Ulna with EI are also presented here, as the EI should be related to the whole bone strength. Three correlations are presented here, two of them are significant; however, the third is presented as BMD is the more common measure. The curve of EI vs. total ulna area has the greatest correlation and most significance and is presented in Figure 8. The other significant correlation is with EI^2 and BMC, illustrated in Figure 9. Total BMD did not correlate significantly with EI, as presented in Figure 10.

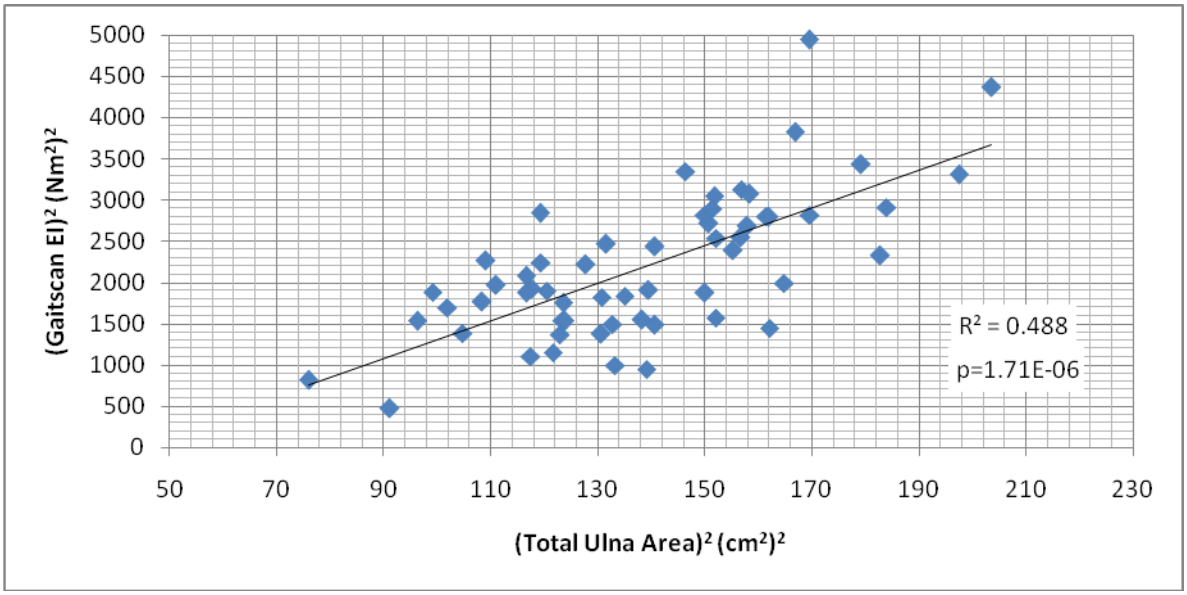

Figure 8 - Correlation between EI^2 and $(\text{Total Ulna Area})^2$

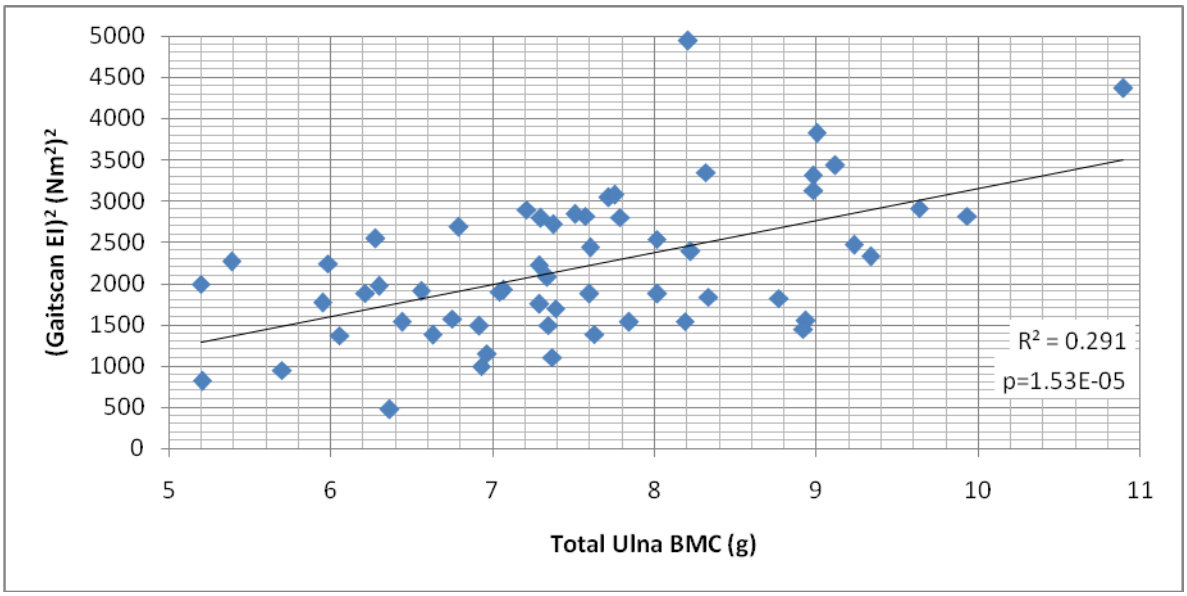

Figure 9 - Correlation between EI^2 and Total Ulna BMC

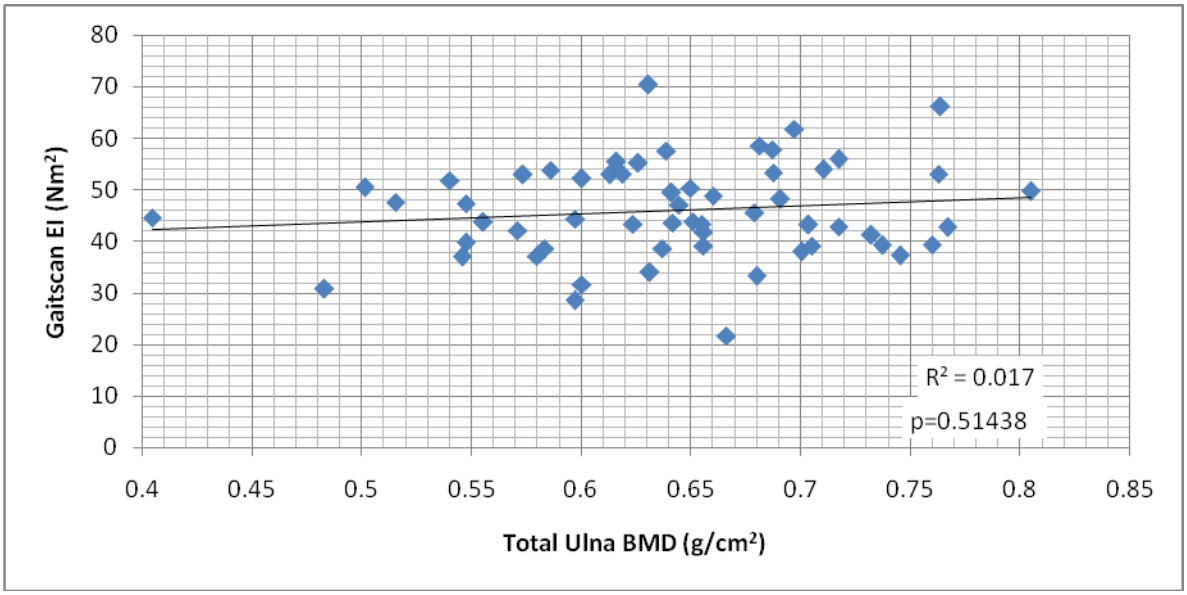

Figure 10 - Correlation between EI and Total BMD (Non-significant)

5.1.4 Correlation with EI and QUS

There were no significant correlations found between the results of the QUS and MRTA EI.

5.1.5 Correlation between Total Ulna BMD and Total Radius BMD

Since the MRTA measure the cross-sectional bending stiffness of the ulna, it would be useful if this was a bone that is frequency used in the diagnosis of osteoporosis; however, typically the radius is used for forearm measurements rather then the ulna. As such, a regression was completed on Total Ulna BMD to Total Radius BMD the two were found to correlate with a p-value of 0.00 and a R^2 value of 0.7202, as illustrated in Figure 11.

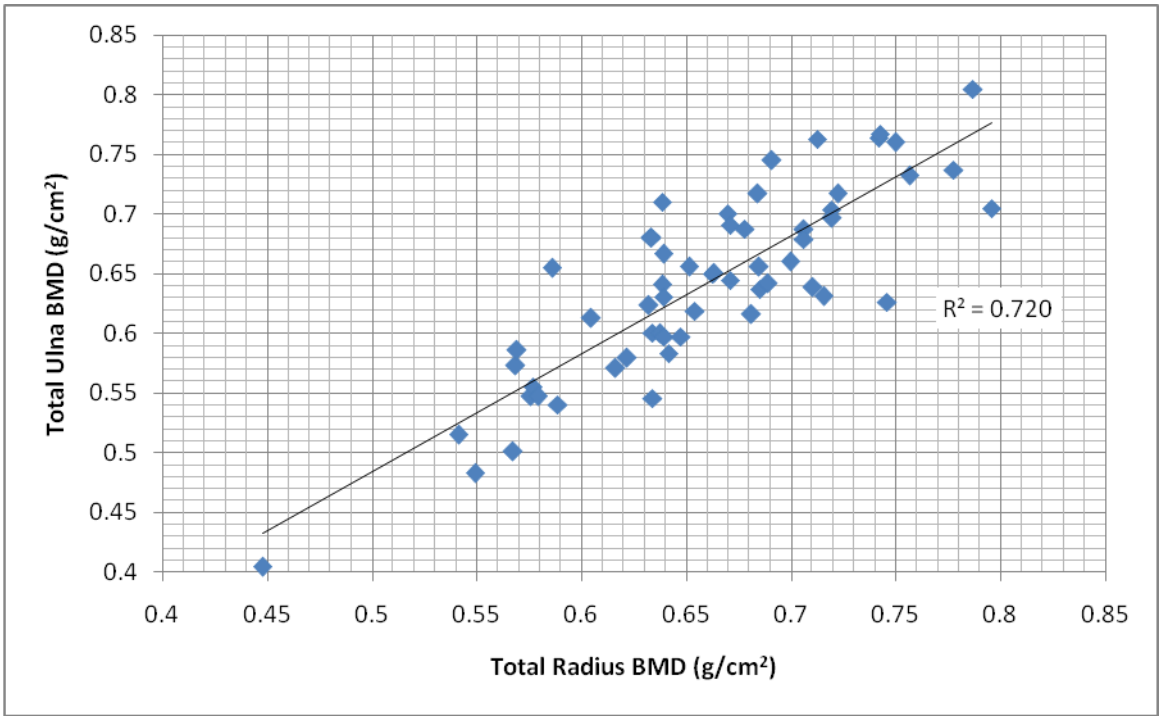

Figure 11 - Correlation between Total Radius BMD and Total Ulna BMD

5.2 Discussion:

5.2.1 EI correlations with age

No significant correlation was found between EI and age of participants. This result was somewhat expected, as a person's age does not define their bone quality. However, the linear regression does have a negative slope as expected, indicating that as a person gets older the EI decreases.

5.2.2 EI correlations with DXA

The correlations with EI was lower than expected based on previous papers. Table 5 illustrates how the BMC to EI correlations of the current study seem to be on the lower of the spectrum of previous correlations of direct linear relationship (no squared variables).

Table 5 - Current Study BMC to EI results in relation to BMC to EI correlations of previous studies

Study	BMC Location	r Value (p value)
Steele, 1988	Total Radius BMC	r=0.82
Myburgh, 1992	Total Ulna BMC	r=0.78 (p= 0.0005)
Djokoto, 2004	Midspan Ulna BMC	r=0.777 (p<0001)
McCabe, 1993	Total Ulna BMC	r=0.72, (p<0.002)
Myburgh, 1993	Total Ulna BMC	r=0.69 (p<0.0001)
Current Study	**1/3 Ulna BMC**	**r=0.605**
McCabe, 1994	Total Ulna BMC	r=0.60 (p<0.02)
Kiebzak, 2005	Total Ulna BMC	r=0.597
McCabe, 1991	Total Ulna BMC	r=0.59 (p<0.02)
Current Study	**1/3 Radius BMC**	**r=0.588**
Ernst, 1988	Total Radius BMC	r=0.58 (p<0.001)
Current Study	**Midspan Radius BMC**	**r=0.535 (non significant)**
Current Study	**Total Radius BMC**	**r=0.535 (non significant)**
Current Study	**Total Ulna BMC**	**r=0.534 (non significant)**
McCabe, 1992	Total Ulna BMC	r=0.52 (p=0.02)
Current Study	**Midspan Ulna BMC**	**r=0.513 (non significant)**
Ernst, 1989	Total Radius BMC	r=0.47 (p<0.01)

Additionally, a comparison to three previous studies that looked at MRTA EI and BMD is presented in Table 6.

Table 6 - Current Study BMD to EI correlations compared to previous study BMD to EI correlations

Study	BMD Location	r Value (p value)
Djokoto, 2004	Midspan Ulna BMD	0.623 (p<0.001)
Kiebzak, 2005	Total Ulna BMD	0.349
Current Study	**1/3 Ulna BMD**	**0.213 (non-significant)**
Current Study	**1/3 Radius BMD**	**0.192 (non-significant)**
Current Study	**Total Ulna BMD**	**0.131 (non-significant)**
Current Study	**Midspan Ulna BMD**	**0.117 (non-significant)**
Current Study	**Total Radius BMD**	**0.0828 (non-significant)**
Current Study	**Midspan Radius BMD**	**0.0307 (non-significant)**
Liang, 2005	Midspan ulna BMD	Non Significant

Here, much similar results were found to Liang et al., in which we found no significant relationships between BMD and EI (for direct linear relationships between the original variables). Never the less, significant relationships between EI and BMD do exist, as presented in Table 4 on page 30. However, these relationships are not simple linear correlations.

The causality for why these large variations in correlations exist is difficult to speculate, however the two technologies are not measuring the same thing, so it's difficult to compare them. Both are ideally trying to get at bone strength or some element of fracture prediction. However, since we cannot measure this in vivo, the correlation between the two at least provides some insight to the amount of similarities that the two technologies capture.

In the paper by Djokoto et al., 2004, the author describes how they went to great lengths to improve the stiffness of the MRTA frame, adding clamps and supports to the frame. It is noted that the correlation between the DXA and MRTA in these cases correlated much better. As such, by improving the supports which support the arm, it may improve the accuracy of the results improving the correlation to a similar level.

5.2.2.1 EI and QUS

None of the values between EI and the QUS measurements had significant correlations. However, this is somewhat expected as the ulna and calcaneous are two different bones in different regions of the body. Firstly, the calcaneous is highly cancellous bone, and as previously mentioned is usually around 95%

cancellous bone, where as the ulna is up to 95% cortical bone. Additionally, the calcaneous is a load being bone being part of walking, where as the ulna is not. As such, it's expected that the two structures would be quite different and not correlate as well. Additionally, as outlined above, if the MRTA structure was reinforced it could provide more reliable results and potentially better correlations.

5.2.3 Correlation between Ulna and Radius

Previously Wilson (1977) found the correlation of BMD in the radius and ulna to be r=0.93. This is similar to the value of r=0.85 that was found in this study. As such, when comparing results from the MRTA, these could potentially be correlated to the Radius BMD rather then Ulna BMD, as Ulnar BMD is not a common measure.

Chapter 6 Development of the Osteoporosis Assessment of Skeletal Integrity System (OASIS)

6.1 Background

Previous work using the MRTA has found that the MRTA has several drawbacks and further work is needed before it can be a successful clinical tool (Djokoto et al., 2004). Additionally, the identification of critical flaws is evident in the failure of the startup company, Gaitscan, which produced approximately 12 MRTA devices before its demise. Since the MRTA devices were designed to be a clinical build, the exact manner in which they operate is unknown due to multilayered circuit

boards and compiled software. As such, our research group has begun investigating an improved MRTA system to be called OASIS.

6.2 Objective

A large portion of this thesis was the initiation of the development of the new OASIS system. The ultimate goal of the project is to develop a fully functional independent system to quantify bone strength more precisely than DXA or QUS. However, due to time restrictions, the objectives for this thesis were to develop the initial hardware and software and investigate the procedure needed to provide relevant results. Presented here is the basic configuration that has been developed in the OASIS system.

6.3 Hardware setup

6.3.1 Components

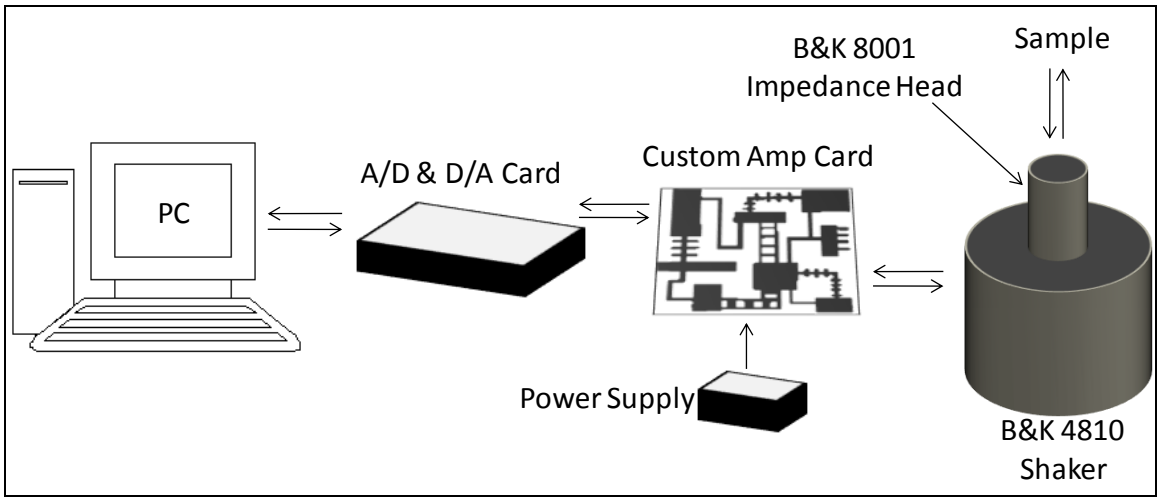

Figure 12 - Hardware setup for OASIS

As illustrated in Figure 12, the components of the OASIS are rather basic. It comprises a PC computer (Dell OptiPlex 755), A/D & D/A Card (USB, 2527;

Measurement computing, Norton, MA), A custom fabricated amplification card with power supply, and a Shaker and Impedance Head (4810 & 8001, Bruel & Kjaer, Denmark). The PC in our setup is the main processing unit, supporting LabVIEW 8.5.1 (National Instruments, Austin TX) it acts as the main interface between the operator and the system. The software generates all input waves and processes all the raw data and provides the necessary user interface. The A/D & D/A card is a standard off the shelf card that allows us to interface with the custom designed analog card much easier. Readily available subVIs for LabVIEW were available for the board making it easier to integrate into the system. The Bruel & Kajaer shaker is an electromagnetic shaker that provides the linear excitation to the sample we are measuring. The shaker is coupled with a Bruel & Kajaer 8001 impedance head, which measures the force and acceleration applied to the sample. The impedance sensor utilizes piezoelectric crystal technology, requiring the charge generated to be transduced to voltage. The impedance sensor was selected because piezoelectrics perform better under high vibration conditions then standard strain gauge sensors. This help to improve the performance and reduce the noise that would be produced from standard sensors. It should be noted however, that increased vibration of the wires can cause additional noise to the signal and vibration of the wires should be minimized. Additionally, high gauge shielded coaxial cables are used to bring the charge signal to the sensor with minimal noise.

6.3.2 Custom Designed Circuit Board

The custom design amplification board serves two purposes: the amplification of the signal to the shaker, and the transduction and amplification of the piezoelectric signal from the impedance sensor. The main component for the amplification of the signal to the shaker is a Brown-Burr OPA549 (Texas Instruments, Dallas TX.) which is a high voltage, high current operational amplifier. A 30KΩ resister was used to establish a current limit of approximately 2.5 amps to prevent damage to the electromagnetic shaker. Additionally, an electronic switch was utilized to prevent accidental amplification when it is not supposed to occur. The resistor configuration was designed to provide a gain of -10. However, the amplifier is required more so to provide the high current needed to power the shaker.

Piezoelectric crystals change in capacitance with certain loading conditions. However, their response has a fall off to it, such that it is primarily applicable to vibration responses. As such, a charge amplifier was needed to convert this small charge produced by the sensors. After the evaluation of many components, the AD743 (Analog Devices, Norwood MA) was selected because it is an ultra low noise, precision, FET input with high impedance suitable for use in piezoelectronics. The circuit was designed such that the amplification would be within the ±10 volts needed to be read by the A/D card.

The force and acceleration signals were calibrated over a series of masses ranging from 0 to slightly greater than 500g. A 120Hz sine wave was used as the stimulus for the shaker. Force signal was divided by the acceleration at the

±peaks of acceleration signal and averaged for the 10 second acquisition. These values were plotted against the know masses to yield a calibration curve.

The stimulus signal is created by creating a signal that has amplitude continuous across the frequency spectrum from 40 Hz to 2000 Hz. This ensures that the magnitude across the frequency to be analyzed is consistent. The signal is outputted at a rate of 10000 samples per second and the force/acceleration signal is sampled at the same rate. Since we are concerned with collecting the complex impedance, acceleration needs to be converted to displacement. Once the FFT has been taken of the acceleration signal, the processed complex signal can be divided by $-4\pi^2f^2$, where f is the frequency, to yield the complex FFT of displacement. The complex force is then divided by the complex displacement yielding the real and imaginary transfer functions. These functions can be processed the same as those from the MRTA.

6.4 Results:

A typical real and imaginary transfer function for a 325mm rod using the new OASIS system is illustrated in Figure 13. The first natural frequency can be noted at approximately 265Hz, whereas the second natural frequency can be seen around 880 Hz.

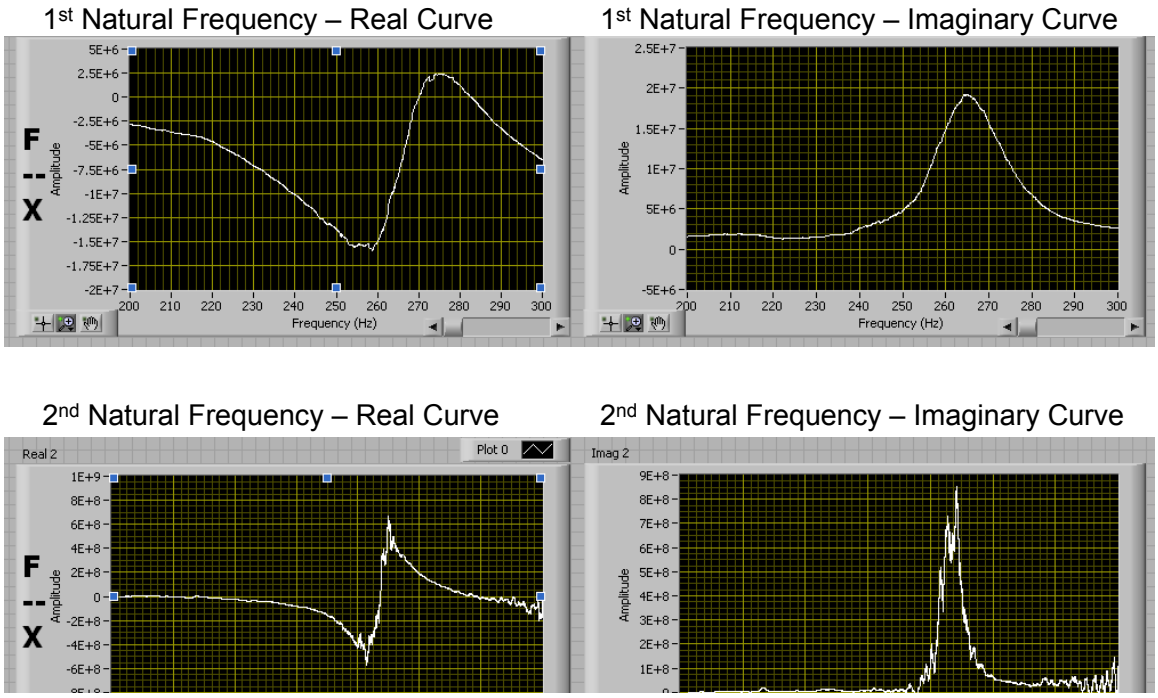

Figure 13 - Real and Imaginary stiffness transfer function for 325mm Aluminum Rod using the OASIS system at the first and second natural frequency.

To determine the natural frequencies for a simply supported beam of uniform cross section, the following formula can be used:

$$\omega_i = \left(\frac{i \cdot \pi}{l}\right)^2 \sqrt{\frac{EI}{\rho \cdot A_{cr}}}$$

where ω_i is the angular frequency at which the i^{th} mode of natural frequency occurs, *l* is the length of the beam, EI is the cross sectional bending stiffness, ρ is the density, and A_{cr} is the cross-sectional area of the beam. By dividing the angular frequency by 2π, the frequency in Hertz can be obtained. The results for the first and second natural frequencies of the beam, in which the results are presented in Figure 13, are presented below:

Diameter: 0.01269m
Length: 0.325m
E=70GPa
ρ=2700 kg/m^3
I=1.2530x10^{-9} kg*m^2 (Calculated)
A_{cr}=1.26477x10^{-4} m^2 (Calculated)

$$f_i = \left(\frac{1}{2\pi}\right)\left(\frac{i \cdot \pi}{l}\right)^2 \sqrt{\frac{EI}{\rho \cdot A_{cr}}}$$

$$f_i = \left(\frac{1}{2\pi}\right)\left(\frac{i \cdot \pi}{0.325}\right)^2 \sqrt{\frac{(70 \times 10^9)(1.253 \times 10^{-9})}{2700 \times (1.26477 \times 10^{-4})}}$$

$$f_i = 238.3 \times i^2$$

$$\boldsymbol{f_1 = 238Hz}$$

$$\boldsymbol{f_2 = 953Hz}$$

6.5 Discussion

As presented in the results, the first bending modes present similar results, with 265 Hz being the approximate observation of first mode, and the calculated value around 240Hz. Similarly, the observed second mode of vibration, as illustrated in Figure 13, is approximately 880Hz, similar to the calculated expected frequency of 950 Hz. It is noted that these values are similar, but not exact. It is likely that this discrepancy occurred either due to the imperfections in the fabrication of the rod. The cross section of the rod, though appears consistent actually varies over 0.2 mm throughout the length, which could account for some of the discrepancies. Additionally, the modulus nor density were measured directly, but were just provided by the resaler for the type of aluminum used, and in production these values may not be as precise. Never the less, these values fall

within a 10 percent margin of the expected values. As such, the OASIS configuration appears to be presenting the correct data on initial configuration.

Chapter 7 Recommendations for future work

1. By improving the arm supports for the MRTA it could dramatically improve the precision of the MRTA. This could allow for greater precision which would result in more meaningful correlations. Thus future work should look at potential ways to stiffen the frame and provide sufficiently rigid supports for the arm.
2. The work that has been done on the OASIS has established some of the fundamentals needed for quantification of bone quality, however this work should be continued to developing the OASIS for clinical use. However, by having the OASIS it will provide increasing an increasing number of options to improve the accuracy. Studies could look at signal acquisition time, input signal types, and provide increasing options for post processing. Lastly this will take a lot of the guesswork out that is currently in the MRTA system, as it seems people who use it don't know precisely what it is doing, and to improve the process one must know exactly what is going on.
3. It would be beneficial to continue mechanical studies. Further ex-vivo studies are needed to see how the MRTA/OASIS relates to actual EI as measured in an MTS system, such as an instron. By performing these tests one can do a correlations to see how well the MRTA or OASIS

relates to actual EI, rather than a surrogate such as BMD. Additionally, high fidelity models using something such as ballistics gel could be used to simulate soft tissues.

4. This study had several limitations due to its size of 58 subjects. To improve the quality of the study, it could also include women as well, as they have a greater risk of Osteoporosis. Additionally, the MRTA has primarily been used on women in the past and it could have been calibrated for women than the stronger bones of men. However, more subjects are needed in total to improve the quality. Due to the small size, the data analysis was primarily limited to simple linear regression as there were so few data points. Additionally, with a sufficiently large data set for a number of years, fracture risk could be evaluated to see how the MRTA evaluates an individual's risk of fracture, as this is the primary factor that physicians are trying to establish in osteoporosis.

Chapter 8 References

ALENFELD, F., DIESSEL, E., BREZGER, M., SIEPER, J., FELSENBERG, D. and BRAUN, J., 2000. Detailed analyses of periarticular osteoporosis in rheumatoid arthritis. Osteoporosis International, 11(5), 400-407.

ARNAUD, S.B., STEELE, C.R., ZHOU, L.-., HUTCHINSON, T. and MARCUS, R., 1991. A direct non-invasive measure of long bone strength, Proceedings of the 13th Annual International Conference of the IEEE Engineering in Medicine and Biology Society, startdate 19911031-enddate 19911103, 19910101 1991, Publ by IEEE pp1984-1985.

ASHMAN, R.B., CORIN, J.D. and TURNER, C.H., 1987. Elastic properties of cancellous bone: measurement by an ultrasonic technique. Journal of Biomechanics, 20(10), 979-986.

BLACK, D.M., CUMMINGS, S.R., GENANT, H.K., NEVITT, M.C., PALERMO, L. and BROWNER, W., 1992. Axial and appendicular bone density predict fractures in older women. Journal of bone and mineral research : the official journal of the American Society for Bone and Mineral Research, 7(6), 633-638.

BLACK, D.M., STEINBUCH, M., PALERMO, L., DARGENT-MOLINA, P., LINDSAY, R., HOSEYNI, M.S. and JOHNELL, O., 2001. An assessment tool for predicting fracture risk in postmenopausal women.

BLAKE, G.M. and FOGELMAN, I. 1997. Technical principles of dual energy X-ray absorptiometry. Seminars in nuclear medicine, 27(3), 210-228.

BOGOCH, E.R., ELLIOT-GIBSON, V., BEATON, D.E., JAMAL, S.A., JOSSE, R.G. and MURRAY, T.M., 2006. Effective initiation of osteoporosis diagnosis and treatment for patients with a fragility fracture in an orthopaedic environment. The Journal of Bone and Joint Surgery, 88(1), 25-34.

BONNICK, S.L., 2004. Bone densitometry in clinical practice: application and interpretation. Humana Press.

BOUXSEIN, M. and RADLOFF, S., 1997. Quantitative Ultrasound of the Calcaneus Reflects the Mechanical Properties of Calcaneal Trabecular Bone*. Journal of Bone and Mineral Research, 12, 839-846.

CAMPBELL, J.N.(. and JURIST, J.M.(., 1971. Mechanical impedance of the femur: A preliminary report. Journal of Biomechanics, 4(5, pp. 319-322), October.

CHENG, S., SIPILÄ, S., TAAFFE, D.R., PUOLAKKA, J. and SUOMINEN, H., 2002. Change in bone mass distribution induced by hormone replacement therapy and high-impact physical exercise in post-menopausal women. Bone, 31(1), 126-135.

CHENG, X.G., LOWET, G., BOONEN, S., NICHOLSON, P.H., BRYS, P., NIJS, J. and DEQUEKER, J., 1997. Assessment of the strength of proximal femur in vitro: relationship to femoral bone mineral density and femoral geometry. Bone, 20(3), 213-218.

CHEUNG, A.M. and DETSKY, A.S., 2008. Osteoporosis and Fractures: Missing the Bridge? JAMA: The Journal of the American Medical Association, 299(12), 1468-1470.

CHRISTENSEN, A.B.(., AMMITZBØLL, F.(., DYRBYE, C.(., CORNELISSEN, M.(., CORNELISSEN, P.(. and VAN DER PERRE, G.(., 1986. Assessment of tibial stiffness by vibration testing in situ —I. Identification of mode shapes in different supporting conditions. Journal of Biomechanics, 19(1), 53-60.

COLLIER, R.J.(., NADAV, O.(. and THOMAS, T.G.(., 1982. The mechanical resonances of a human tibia: Part I— In vitro. Journal of Biomechanics, 15(8), 545-553.

CUMMINGS, S.R., NEVITT, M.C., BROWNER, W.S., STONE, K., FOX, K.M., ENSRUD, K.E., CAULEY, J., BLACK, D. and VOGT, T.M., 1995. Risk factors for hip fracture in white women. New England Journal of Medicine, 332(12), 767-774.

CUMMINGS, S.R., BLACK, D.M., NEVITT, M.C., BROWNER, W., CAULEY, J., ENSRUD, K., GENANT, H.K., PALERMO, L., SCOTT, J. and VOGT, T.M., 1993. Bone density at various sites for prediction of hip fractures. The Study of Osteoporotic Fractures Research Group. Lancet, 341(8837), 72-75.

CUMMINGS, S.R., KARPF, D.B., HARRIS, F., GENANT, H.K., ENSRUD, K., LACROIX, A.Z. and BLACK, D.M., 2002. Improvement in spine bone density and reduction in risk of vertebral fractures during treatment with antiresorptive drugs.

CUMMINGS, S.R. and MELTON, L.J., 2002. Epidemiology and outcomes of osteoporotic fractures. The Lancet, 359(9319, pp. 1761-1767), May.

CURREY, J.D., 1990. Physical characteristics affecting the tensile failure properties of compact bone. Journal of Biomechanics, 23(8), 837-844.

DJOKOTO, C., TOMLINSON, G., WALDMAN, S., GRYNPAS, M. and CHEUNG, A.M., 2004. Relationship among MRTA, DXA, and QUS. Journal of clinical densitometry : the official journal of the International Society for Clinical Densitometry, 7(4), 448-456.

DUQUETTE, J., HONEYMAN, T., HOFFMAN, A., AHMADI, S. and BARAN, D., 1997. Effect of bovine bone constituents on broadband ultrasound attenuation measurements. Bone, 21(3), 289-294.

EARNSHAW, S.A., CAWTE, S.A., WORLEY, A. and HOSKING, D.J., 1998. Colles' fracture of the wrist as an indicator of underlying osteoporosis in postmenopausal women: A prospective study of bone mineral density and bone turnover rate.

ERNST, A., MINNE, H.W., ZIMMERMANNS, V., BACHER, T., STAHL, R., STEELE, C.R. and & ZIEGLER, R., 1988. Mechanical resonance tissue analysis applied to determine bone stiffness in normal humans and patients with metabolic bone disease. Calcified tissue international, 44(J11), S59.

ETTINGER, B., BLACK, D.M., MITLAK, B.H., KNICKERBOCKER, R.K., NICKELSEN, T., GENANT, H.K., CHRISTIANSEN, C., DELMAS, P.D., ZANCHETTA, J.R., STAKKESTAD, J., GLÜER, C.C., KRUEGER, K., COHEN, F.J., ECKERT, S., ENSRUD, K.E., AVIOLI, L.V., LIPS, P. and CUMMINGS, S.R., 1999. Reduction of vertebral fracture risk in postmenopausal women with osteoporosis treated with raloxifene: results from a 3-year randomized clinical trial. Multiple Outcomes of Raloxifene Evaluation (MORE) Investigators. JAMA : the journal of the American Medical Association, 282(7), 637-645.

FISHER, JOHN P., AEGEAN CONFERENCES, 2006. Tissue engineering. Springer.

FITZPATRICK, L.A., 2002. Secondary causes of osteoporosis, Mayo Clinic Proceedings, 2002, MAYO FOUNDATION pp453-468.

FOGELMAN, I. and BLAKE, G.M., 2000. Different approaches to bone densitometry. The Journal of nuclear medicine, 41(12), 2015-2025.

FRANKE, E.K., 1956. Response of the Human Skull to Mechanical Vibrations. The Journal of the Acoustical Society of America, 28(6), 1277.

FRANKE, E.K., 1952. The Impedance of the Human Mastoid. The Journal of the Acoustical Society of America, 24(4), 410.

FRANKE, E.K., 1951. Mechanical impedance of the surface of the human body. Journal of Applied Physiology, 3(10), 582-590.

FROST, H.M., 2003. Bone's mechanostat: a 2003 update. The anatomical record.Part A, Discoveries in molecular, cellular, and evolutionary biology, 275(2), 1081-1101.

GARDNER, M.J., BROPHY, R.H., DEMETRAKOPOULOS, D., KOOB, J., HONG, R., RANA, A., LIN, J.T. and LANE, J.M., 2005. Interventions to Improve Osteoporosis Treatment Following Hip Fracture A Prospective, Randomized Trial. The Journal of Bone and Joint Surgery, 87(1), 3-7.

GLÜER, C.C., 1997. Quantitative ultrasound techniques for the assessment of osteoporosis: expert agreement on current status. Journal of Bone and Mineral Research, 12, 1280-1288.

GOLD, D.T. and SILVERMAN, S.L., 2004. CME Osteoporosis Self-management: Choices For Better Bone Health. Southern medical journal, 97(6), 551.

HAN, S., RHO, J., MEDIGE, J. and ZIV1, I., 1996. Ultrasound velocity and broadband attenuation over a wide range of bone mineral density. Osteoporosis International, 6(4), 291-296.

HOCHBERG, M.C., GREENSPAN, S., WASNICH, R.D., MILLER, P., THOMPSON, D.E. and ROSS, P.D., 2002. Changes in bone density and turnover explain the reductions in incidence of nonvertebral fractures that occur during treatment with antiresorptive agents.

HODGSKINSON, R., NJEH, C., WHITEHEAD, M. and LANGTON, C., 1996. The non-linear relationship between BUA and porosity in cancellous bone. Physics in Medicine and Biology, 41(11), 2411-2420.

HODGSON, V.R.(., NAKAMURA, M.S.(. and NAKAMURA, G.S.(., 1968. Mechanical impedance and impact response of the human cadaver zygoma. Journal of Biomechanics, 1(2, pp. 73-78), July.

HUTCHINSON, T.M., BAKULIN, A.V., RAKHMANOV, A.S., MARTIN, R.B., STEELE, C.R. and ARNAUD, S.B., 2001. Effects of chair restraint on the strength of the tibia in rhesus monkeys. Journal of medical primatology, 30(6), 313-321.

JERGAS, M. and GLUER, C.C., 1997. Assessment of fracture risk by bone density measurements. Seminars in nuclear medicine, 27(3), 261-275.

JURIST, J.M.(. and FOLTZ, A.S.(., 1977. Human ulnar bending stiffness, mineral content, geometry and strength. Journal of Biomechanics, 10(8), 455-459.

JURIST, J.M.(. and KIANIAN, K., 1973. Three models of the vibrating ulna. Journal of Biomechanics, 6(4, pp. 331-342), July.

KACZMAREK, M., PAKUŁA, M. and KUBIK, J., 2000. Multiphase nature and structure of biomaterials studied by ultrasounds. Ultrasonics, 38(1-8), 703-707.

KANIS, J.A., 1994. Assessment of fracture risk and its application to screening for postmenopausal osteoporosis: synopsis of a WHO report. WHO Study Group. Osteoporosis international : a journal established as result of cooperation between the European Foundation for Osteoporosis and the National Osteoporosis Foundation of the USA, 4(6), 368-381.

KARLSSON, M.K., JOHNELL, O., NILSSON, B.E., SERNBO, I. and OBRANT, K.J., 1993. Bone mineral mass in hip fracture patients. Bone, 14(21), 161-165.

KASTURI, G.C., CIFU, D.X. and ADLER, R.A., 2009. A Review of Osteoporosis: Part I. Impact, Pathophysiology, Diagnosis and Unique Role of the Physiatrist. PM&R, 1(3), 254-260.

KIEBZAK, G.M. and AMBROSE, C.G., 2005. Relationship among MRTA, DXA, and QUS revisited. Journal of clinical densitometry : the official journal of the International Society for Clinical Densitometry, 8(4), 396-403.

LAFORTUNE, M.A.(., LAKE, M.J.(. and HENNIG, E., 1995. Transfer function between tibial acceleration and ground reaction force. Journal of Biomechanics, 28(1, pp. 113-117), January.

LANGTON, C., NJEH, C., HODGSKINSON, R. and CURREY, J., 1996. Prediction of mechanical properties of the human calcaneus by broadband ultrasonic attenuation. Bone, 18(6), 495-503.

LEWIS, J.L.(., 1975. A dynamic model of a healing fractured long bone. Journal of Biomechanics, 8(1), 17-25.

LIANG, M.T.C.(., ARNAUD, S.B.(., STEELE, C.R.(.,3), HATCH, P. and MORENO, A.,2), 2005. Ulnar and tibial bending stiffness as an index of bone strength in synchronized swimmers and gymnasts. European journal of applied physiology, 94(4, pp. 400-407), July.

LOWET, G.(., DAYUAN, X.(. and VAN DER PERRE, G.(., 1996. Study of the vibrational behaviour of a healing tibia using finite element modelling. Journal of Biomechanics, 29(8, pp. 1003-1010), August.

MARSHALL, D., JOHNELL, O. and WEDEL, H., 1996. Meta-analysis of how well measures of bone mineral density predict occurrence of osteoporotic fractures. BMJ (Clinical research ed.), 312(7041), 1254-1259.

MARTIN, R.B. and ISHIDA, J., 1989. The relative effects of collagen fiber orientation, porosity, density, and mineralization on bone strength. Journal of Biomechanics, 22(5), 419-426.

MARTIN, R.B., 1991. Determinants of the mechanical properties of bones. Journal of Biomechanics, 24, 79-88.

MAUCK, K.F. and CLARKE, B.L., 2006. Diagnosis, screening, prevention, and treatment of osteoporosis, Mayo Clinic Proceedings, 2006, Mayo Clinic pp662.

MAYHEW, P.M., THOMAS, C.D., CLEMENT, J.G., LOVERIDGE, N., BECK, T.J., BONFIELD, W., BURGOYNE, C.J. and REEVE, J., 2005. Relation between age, femoral neck cortical stability, and hip fracture risk. Lancet, 366(9480), 129-135.

MCCABE, F., ZHOU, L.J., STEELE, C.R. and MARCUS, R., 1991. Noninvasive assessment of ulnar bending stiffness in women. Journal of bone and mineral research : the official journal of the American Society for Bone and Mineral Research, 6(1), 53-59.

MILLER, L.E., WOOTTEN, D.F., NICKOLS-RICHARDSON, S.M., RAMP, W.K., STEELE, C.R., COTTON, J.R., CARNEAL, J.P. and HERBERT, W.G., 2007. Isokinetic training increases ulnar bending stiffness and bone mineral in young women. Bone, 41(4), 685-689.

MILLER, L.E., NICKOLS-RICHARDSON, S.M., WOOTTEN, D.F., RAMP, W.K., STEELE, C.R., COTTON, J.R., CARNEAL, J.P. and HERBERT, W.G., 2009. Isokinetic resistance training increases tibial bending stiffness in young women. Calcified tissue international, 84(6), 446-452.

MILLER, P.D., BARLAS, S., BRENNEMAN, S.K., ABBOTT, T.A., CHEN, Y.T., BARRETT-CONNOR, E. and SIRIS, E.S., 2004. An approach to identifying osteopenic women at increased short-term risk of fracture.

MUNDINGER, A., WIESMEIER, B., DINKEL, E., HELWIG, A., BECK, A. and SCHULTE MOENTING, J., 1993. Quantitative image analysis of vertebral body

architecture--improved diagnosis in osteoporosis based on high-resolution computed tomography. The British journal of radiology, 66(783), 209-213.

MYBURGH, K.H., 1993. Influence Of Recreational Activity And Muscle Strength On Ulnar Bending Stiffness In Men. Medicine and science in sports, 25, 592-596.

MYBURGH, K.H., ZHOU, L.J., STEELE, C.R., ARNAUD, S. and MARCUS, R., 1992. In vivo assessment of forearm bone mass and ulnar bending stiffness in healthy men. Journal of bone and mineral research : the official journal of the American Society for Bone and Mineral Research, 7(11), 1345-1350.

NEVITT, M.C., JOHNELL, O., BLACK, D.M., ENSRUD, K., GENANT, H.K. and CUMMINGS, S.R., 1994. Bone mineral density predicts non-spine fractures in very elderly women. Study of Osteoporotic Fractures Research Group. Osteoporosis international : a journal established as result of cooperation between the European Foundation for Osteoporosis and the National Osteoporosis Foundation of the USA, 4(6), 325-331.

NICHOLSON, P., HADDAWAY, M. and DAVIE, M., 1994. The dependence of ultrasonic properties on orientation in human vertebral bone. Physics in Medicine and Biology, 39(6), 1013-1024.

NICHOLSON, P. and NJEH, C., 1999. Ultrasonic studies of cancellous bone in vitro. Quantitative ultrasound: Assessment of osteoporosis and bone status.London: Martin Dunitz, , 195-219.

NJEH, C., FUERST, T., DIESSEL, E. and GENANT, H., 2001. Is quantitative ultrasound dependent on bone structure? A reflection. Osteoporosis International, 12(1), 1-15.

NJEH, C., HODGSKINSON, R., CURREY, J. and LANGTON, C., 1996. Orthogonal relationships between ultrasonic velocity and material properties of bovine cancellous bone. Medical Engineering and Physics, 18(5), 373-381.

NORRDIN, R.W.(., SIMSKE, S.J.(., GAARDE, S.(., SCHWARDT, J.D.(. and THRALL, M.A., 1995. Bone Changes in Mucopolysaccharidosis VI in Cats and the Effects of Bone Marrow Transplantation: Mechanical Testing of Long Bones. Bone, 17(5, pp. 485-489), November.

NOYES, D.H., CLARK, J.W. and WATSON, C.E., 1968. Mechanical input impedance of human teeth in vivo. Med.Biol.Engineering, 6, 487-492.

PAIN, H.J., 2005. The Physics of Vibrations and Waves.

PEEL, N., MOORE, D., BARRINGTON, N., BAX, D. and EASTELL, R., 1995. Risk of vertebral fracture and relationship to bone mineral density in steroid treated rheumatoid arthritis. British medical journal, 54(10), 801-806.

RAMNEMARK, A., NYBERG, L., LORENTZON, R., ENGLUND, U. and GUSTAFSON, Y., 1999. Progressive hemiosteoporosis on the paretic side and increased bone mineral density in the nonparetic arm the first year after severe stroke. Osteoporosis International, 9(3), 269-275.

ROBERTS, S.G., HUTCHINSON, T.M., ARNAUD, S.B., KIRATLI, B.J., MARTIN, R.B. and STEELE, C.R., 1996. Noninvasive determination of bone mechanical properties using vibration response: a refined model and validation in vivo. Journal of Biomechanics, 29(1), 91-98.

SAFTIG, P., HUNZIKER, E., WEHMEYER, O., JONES, S., BOYDE, A., ROMMERSKIRCH, W., MORITZ, J.D., SCHU, P. and VON FIGURA, K., 1998. Impaired osteoclastic bone resorption leads to osteopetrosis in cathepsin-K-deficient mice. Proceedings of the National Academy of Sciences, 95(23), 13453-13458.

SAHA, S. and LAKES, R.S.(., 1977. The effect of soft tissue on wave-propagation and vibration tests for determining the in vivo properties of bone. Journal of Biomechanics, 10(7), 393-401.

SCHLENKER, R.A. and VONSEGGEN, W.W., 1976. The distribution of cortical and trabecular bone mass along the lengths of the radius and ulna and the implications forin vivo bone mass measurements. Calcified tissue international, 20(1), 41-52.

SCHOTT, A.M., CORMIER, C., HANS, D., FAVIER, F., HAUSHERR, E., DARGENT-MOLINA, P., DELMAS, P.D., RIBOT, C., SEBERT, J.L., BREART, G. and MEUNIER, P.J., 1998. How Hip and Whole-Body Bone Mineral Density Predict Hip Fracture in Elderly Women: The EPIDOS Prospective Study. Osteoporosis International, 8(3), 247-254.

SERPE, L. and RHO, J.Y., 1996. The nonlinear transition period of broadband ultrasound attenuation as bone density varies. Journal of Biomechanics, 29(7), 963-966.

SIRIS, E.S., CHEN, Y.T., ABBOTT, T.A., BARRETT-CONNOR, E., MILLER, P.D., WEHREN, L.E. and BERGER, M.L., 2004. Bone mineral density thresholds for pharmacological intervention to prevent fractures.

STEELE, C.R., ZHOU, L.J., GUIDO, D., MARCUS, R., HEINRICHS, W.L. and CHEEMA, C., 1988. Noninvasive determination of ulnar stiffness from mechanical response--in vivo comparison of stiffness and bone mineral content in humans. Journal of Biomechanical Engineering, 110(2), 87-96.

STONE, K.L., SEELEY, D.G., LUI, L.Y., CAULEY, J.A., ENSRUD, K., BROWNER, W., NEVITT, M.C., CUMMINGS, S.R. and OSTEOPOROTIC FRACTURES RESEARCH, 2003. BMD at multiple sites and risk of fracture of multiple types: Long-term results from the study of osteoporotic fractures.

STUSSI, E., BISCHOF, H.J., LUCCHINETTI, E., HERZOG, R., GERBER, H., KRAMERS, I., STALDER, H., KRIEMLER, S., CASEZ, P. and JAGEN, P., 1994. Entwicklung und Anpassung der Biegesteiligkeit des Extremitiitenskelettes durch Training am Beispiel der Tibia [Development and adaptation of bending stiffness of the skeleton of the extremities as exemplified by the human tibia through exercise]. Sportverl Sportschad, 8, 103-110.

TABENSKY, A.D., WILLIAMS, J., DELUCA, V., BRIGANTI, E. and SEEMAN, E., 1996. Bone mass, areal, and volumetric bone density are equally accurate, sensitive, and specific surrogates of the breaking strength of the vertebral body: an in vitro study. Journal of bone and mineral research : the official journal of the American Society for Bone and Mineral Research, 11(12), 1981-1988.

THOMPSON, G.A.(., YOUNG, D.R.(. and ORNE, D.(., 1976. In vivo determination of mechanical properties of the human ulna by means of mechanical impedance tests: experimental results and improved mathematical model. Med.Biol.Engineering, 14(3), 253-262.

VAN DER PERRE, G. and LOWET, G., 1996. In vivo assessment of bone mechanical properties by vibration and ultrasonic wave propagation analysis. Bone, 18(1), 29-35.

VIGUET-CARRIN, S., GARNERO, P. and DELMAS, P.D., 2006. The role of collagen in bone strength. Osteoporosis International, 17(3), 319-336.

WACHTER, N.J., KRISCHAK, G.D., MENTZEL, M., SARKAR, M.R., EBINGER, T., KINZL, L., CLAES, L. and AUGAT, P., 2002. Correlation of bone mineral density with strength and microstructural parameters of cortical bone in vitro. Bone, 31(1), 90-95.

WAINWRIGHT, S.A., MARSHALL, L.M., ENSRUD, K.E., CAULEY, J.A., BLACK, D.M., HILLIER, T.A., HOCHBERG, M.C., VOGT, M.T., ORWOLL, E.S. and

STUDY OSTEOPOROTIC FRACTURES RES G, 2005. Hip fracture in women without osteoporosis.

WILSON, C., 1977. Bone-mineral content of the femoral neck and spine versus the radius or ulna. The Journal of Bone and Joint Surgery, 59(5), 665-669.

YOUNG, D.R., HOWARD, W.H., CANN, C. and STEELE, C.R., 1979. Noninvasive measures of bone bending rigidity in the monkey (M. nemestrina). Calcified Tissue International 27(2) 1979:109-115., 27(2), 109-115.

YOUNG, D.R., NIKLOWITZ, W.J. and STEELE, C.R., 1983. Tibial changes in experimental disuse osteoporosis in the monkey. Calcified tissue international, 35(3), 304-308.

ZEHNDER, Y., LÜTHI, M., MICHEL, D., KNECHT, H., PERRELET, R., NETO, I., KRAENZLIN, M., ZÄCH, G. and LIPPUNER, K., 2004. Long-term changes in bone metabolism, bone mineral density, quantitative ultrasound parameters, and fracture incidence after spinal cord injury: a cross-sectional observational study in 100 paraplegic men. Osteoporosis International, 15(3), 180-189.

ZERWEKH, J.E., RUML, L.A., GOTTSCHALK, F. and PAK, C.Y.C., 1998. The effects of twelve weeks of bed rest on bone histology, biochemical markers of bone turnover, and calcium homeostasis in eleven normal subjects. Journal of bone and mineral research, 13, 1594-1601.